AD A139893

DAVID W. TAYLOR NAVAL SHIP
RESEARCH AND DEVELOPMENT CENTER

Bethesda, Maryland 20084

BIMETAL AND MULTIMETAL GALVANIC CORROSION

PREDICTION USING LONG- AND SHORT-TERM

POLARIZATION CURVES

by

J.R. Scully

DTIC
ELEC
APR 9 1984

A

SHIP MATERIALS ENGINEERING DEPARTMENT
RESEARCH AND DEVELOPMENT REPORT

February 1984

DTNSRDC/SME-83-85

84 04 06 014

MAJOR DTNSRDC ORGANIZATIONAL COMPONENTS

```
                        ┌─────────────────────────┐
                        │        DTNSRDC          │
                        │      COMMANDER       00 │
                        │  TECHNICAL DIRECTOR     │
                        │                      01 │
                        └─────────────────────────┘

┌──────────────────────┐                    ┌──────────────────────┐
│  OFFICER-IN-CHARGE    │                    │  OFFICER-IN-CHARGE    │
│     CARDEROCK     05  │                    │     ANNAPOLIS     04  │
└──────────────────────┘                    └──────────────────────┘

┌──────────────────────┐
│      SYSTEMS          │
│    DEVELOPMENT        │
│   DEPARTMENT      11  │
└──────────────────────┘

┌──────────────────────┐                    ┌──────────────────────┐
│  SHIP PERFORMANCE     │                    │    AVIATION AND       │
│    DEPARTMENT         │                    │  SURFACE EFFECTS      │
│                  15   │                    │  DEPARTMENT       16  │
└──────────────────────┘                    └──────────────────────┘

┌──────────────────────┐                    ┌──────────────────────┐
│     STRUCTURES        │                    │   COMPUTATION,        │
│    DEPARTMENT         │                    │  MATHEMATICS AND      │
│                  17   │                    │ LOGISTICS DEPARTMENT  │
│                       │                    │                   18  │
└──────────────────────┘                    └──────────────────────┘

┌──────────────────────┐                    ┌──────────────────────┐
│   SHIP ACOUSTICS      │                    │  PROPULSION AND       │
│    DEPARTMENT         │                    │  AUXILIARY SYSTEMS    │
│                  19   │                    │  DEPARTMENT       27  │
└──────────────────────┘                    └──────────────────────┘

┌──────────────────────┐                    ┌──────────────────────┐
│   SHIP MATERIALS      │                    │     CENTRAL           │
│   ENGINEERING         │                    │ INSTRUMENTATION       │
│   DEPARTMENT     28   │                    │  DEPARTMENT       29  │
└──────────────────────┘                    └──────────────────────┘
```

SECURITY CLASSIFICATION OF THIS PAGE *(When Data Entered)*

REPORT DOCUMENTATION PAGE		READ INSTRUCTIONS BEFORE COMPLETING FORM
1. REPORT NUMBER DTNSRDC/SME-83/85	2. GOVT ACCESSION NO. AD-A139893	3. RECIPIENT'S CATALOG NUMBER
4. TITLE *(and Subtitle)* BIMETAL AND MULTIMETAL GALVANIC CORROSION PREDICTION USING LONG- AND SHORT-TERM POLARIZATION CURVES		5. TYPE OF REPORT & PERIOD COVERED
		6. PERFORMING ORG. REPORT NUMBER
7. AUTHOR(s) J.R. Scully		8. CONTRACT OR GRANT NUMBER(s)
9. PERFORMING ORGANIZATION NAME AND ADDRESS David Taylor Naval Ship R&D Center Bethesda, MD 20084		10. PROGRAM ELEMENT, PROJECT, TASK AREA & WORK UNIT NUMBERS Program Element 62761N; Task Area SF 71541-591 Work Unit 2803-163
11. CONTROLLING OFFICE NAME AND ADDRESS Naval Sea Systems Command (SEA 05R25) Washington, DC 20362		12. REPORT DATE February 1984
		13. NUMBER OF PAGES 67
14. MONITORING AGENCY NAME & ADDRESS*(if different from Controlling Office)*		15. SECURITY CLASS. *(of this report)* UNCLASSIFIED
		15a. DECLASSIFICATION/DOWNGRADING SCHEDULE

16. DISTRIBUTION STATEMENT *(of this Report)*

APPROVED FOR PUBLIC RELEASE; DISTRIBUTION UNLIMITED.

17. DISTRIBUTION STATEMENT *(of the abstract entered in Block 20, if different from Report)*

18. SUPPLEMENTARY NOTES

19. KEY WORDS *(Continue on reverse side if necessary and identify by block number)*

Galvanic Corrosion; Galvanic Couple Current, Galvanic Couple Potential Potentiostatic Polarization; Potentiodynamic Polarization; Applied Potential; Galvanic Compatibility; Short-Term Exposure; Long-Term Exposure; Steady-State Corrosion Rate

20. ABSTRACT *(Continue on reverse side if necessary and identify by block number)*

Long-term potentiostatic polarization curves of up to 120-days duration were developed for the following materials: (1) 90-10 copper-nickel (C70600); (2) Monel 400 (N04400); (3) Inconel 625 (N06625); (4) Navy M-bronze (C92200); (5) nickel-aluminum-bronze (95800); and (6) HY-80 steel. In addition, potentiostatic polarization curves have been developed for Titanium-50 (R50400), 70-30 copper-nickel (C71500), and anode grade zinc (MIL-STD-18001). Also, ⟶

(Continued on reverse side)

DD FORM 1473 EDITION OF 1 NOV 65 IS OBSOLETE
1 JAN 73
S/N 0102-014-6601 |

(Block 20 continued)

short-term potentiodynamic polarization curves were developed at four
scan rates and two pre-exposure levels on specimens of all but the last
three of the above materials. The scan rates utilized ranged from 0.5 to
100 volts/hour and pre-exposure times were 1 hour and 120 days. Long-
term potentiostatic data was used to predict the behavior of actual two
and three metal couples. The predictions had a level of accuracy equal
to, or superior than, the conventional galvanic corrosion prediction
techniques utilizing galvanic corrosion rate tables or corrosion poten-
tial differences. Potentiodynamic data from 120-day pre-exposed, low
scan rate tests has demonstrated some utility in predicting bimetal
couple behavior.

Accession For

NTIS
DTIC
U
I

TABLE OF CONTENTS

LIST OF FIGURES

LIST OF TABLES

ABSTRACT

Long-term potentiostatic polarization curves of up to 120-days duration were developed for the following materials: (1) 90-10 copper-nickel (C70600); (2) Monel 400 (N04400); (3) Inconel 625 (N06625); (4) Navy M-bronze (C92200); (5) nickel-aluminum bronze (95800); and (6) HY-80 steel. In addition, potentionstatic polarization curves have been developed for titanium-50 (R50400), 70-30 copper-nickel (C71500), and anode grade zinc (MIL-STD-18001). Also, short-term potentiodynamic polarization curves were developed at four scan rates and two pre-exposure levels on specimens of all but the last three of the above materials. The scan rates utilized ranged from 0.5 to 100 volts/hour and pre-exposure times were 1 hour and 120 days. Long-term potentiostatic data was used to predict the behavior of actual two and three metal couples. The predictions had a level of accuracy equal to, or superior than, the conventional galvanic corrosion prediction techniques utilizing galvanic corrosion rate tables or corrosion potential differences. Potentiodynamic data from 120-day pre-exposed, low-scan-rate tests has demonstrated some utility in predicting bimetal couple behavior.

ADMINISTRATIVE INFORMATION

INTRODUCTION

The tendencies toward galvanic corrosion in seawater is conventionally estimated using tables of galvanic compatibility,[1] or differences in corrosion potential between members of the galvanic couple, where the corrosion potentials are obtained from a galvanic series.[2] Galvanic corrosion rates can also be directly measured by performing galvanic couple exposures, where two or more alloys are electrically shorted through zero resistance ammeters or 1 ohm resistors. Weight losses or galvanic currents are then measured versus time. The latter technique has been utilized by the Center on numerous occasions to study galvanic compatibility.[3,4]

---

*A complete list of references is given on page 61.

Tables of galvanic compatibility are qualitative, providing only an indication of the possibility for corrosion damage in the galvanic couple. Couple exposures, although accurate, are both expensive and time-consuming, and provide only quantitative predictive capability for the specific conditions tested, i.e. seawater composition, temperature, velocity, anode to cathode area ratio, and geometry. Couple exposure data developed for one purpose can seldom be applied to a different galvanic situation, and new exposures are usually necessary for every situation encountered. Further, a galvanic couple exposure of alloys A and B provides no information on compatibility when alloy C is introduced, unless that actual exposure is also performed. In other words, only very specific information on corrosion characteristics is obtained.

The use of electrochemical methods to predict galvanic corrosion has been previously described.[5-8] First, polarization curves, which are plots of the log of current density as a function of applied potential, are empirically obtained for the materials involved. Current originating at the anode of a galvanic couple must equal the current received at the cathode, i.e. the rate of oxidation must equal the rate of reduction. Thus, if the polarization curves for two materials forming a galvanic couple are normalized with respect to wetted surface area and superimposed, the intersection of the anodic (positive) curve of one material with the cathodic (negative) curve of the other will define the magnitude and direction of current in the galvanic couple and the couple potential.* Metal loss of the anode material can then be calculated from the couple current by the use of Faraday's Law. This calculation may not be exact, however, because the couple current measured is actually the difference between the actual anodic corrosion current, giving rise to dissolution and the cathodic current generated by the presence of some cathodic reactions on the anode. However, net anodic and cathodic currents can be readily studied for each material. Thus, true corrosion rate can be exactly predicted only if one also has a calculated or empirically obtained relationship between applied potential and corrosion rate based on weight loss for the materials involved.

Galanic couple studies performed both at the Center and elsewhere have demonstrated that galvanic couple potential and current behavior in seawater can change

---

*In theory, the same procedure can be utilized to study a multimetal galvanic couple consisting of three or more alloys coupled together.

considerably over periods of up to 120 days as passive films, corrosion products, and calcareous deposits form, and as the concentrations of anodic and cathodic species in solution stabilize. Thus, to adequately predict long-term galvanic behavior, long-term data is desired. Long-term behavior can be approximated by exposing a series of specimens of each material in the couple, each at a different but constant potential; and by monitoring the applied current until it stabilizes. This process can require 120 days or exposure or longer. Plotting applied potential against the stable current value for each specimen yields a series of points defining the long-term potentiostatic polarization curve for the material. By subtracting weight loss information obtained from short-term exposures, the steady-state corrosion rate over the latter portion of the exposure, which approximates long-term behavior, can be obtained as a function of applied potential. Use of long-term potentiostatic polarization curves derived in this manner can allow quantitative prediction of galvanic corrosion behavior to the extent that the environment can be reproduced, assuming that galvanic couples can be considered as having a constant potential. Of course, new polarization curves would be required for different conditions of velocity, temperature, dissolved oxygen, etc.

Since a considerable amount of time, material, and apparatus is required for the generation of long-term potentiostatic polarization curves, it is desirable to find a short-term test for each class of material that would approximate long-term potentiostatic behavior. Possibilities include slow-scan-rate potentiodynamic testing, step-potential scanning, short-term potentiostatic testing, and potentiodynamic testing of material which has been pre-exposed to form corrosion product films. Step-galvanostatic and short-term galvanostatic techniques are also possibilities.

The method of obtaining potentiodynamic polarization curves is to continuously scan the potential of freshly-polished surfaces of the material at a fixed rate, while recording the current response of the electrochemical interface. Application of information potentiodynamically obtained in this manner to actual galvanic couples is difficult for a number of reasons. First, the currents measured are a function of the potential scan rate. Faster scan rates may yield higher currents, and the shape of the curves may change with different rates. Second, measured currents may also vary depending on the potential from which the scan was started and on whether the scan was in the anodic or cathodic direction. Thus, the prior potential history of the material affects the results. This is a problem

3

particularly when predicting galvanic couple behavior, since the materials in a galvanic couple are likely to be experiencing a relatively constant potential. Third, most galvanic couples in service are of long duration so that corrosion product films can be formed which affect apparent polarization behavior.[9] In some cases sufficient corrosion has taken place for surface roughening and an increase in electrochemical area to be significant. Finally, ohmic resistance through the electrolyte can influence both couple polarization behavior and scan rate in potentiodynamic tests. These effects are discussed elsewhere.[9,10]

OBJECTIVE

The first objective of this investigation is to develop the capability to quantitatively predict the corrosion behavior of complex galvanic cells (multimetal galvanic assemblies) as well as bimetal couples in any area ratio. This is to be accomplished by both using previously developed long-term potentiostatic polarization data. The second objective is to generate polarization curves which are similar to long-term potentiostatic curves, using short-term polarization methods. Prediction accuracy is to be verified by actual bimetal and multimetal galvanic couple exposures. In addition, long-term potentiostatic polarization data is to be developed for other alloys including anode materials for the prediction of cathodic protection current demands.

Other aspects of this investigation not reported here include quantitative prediction of galvanic corrosion behavior in a geometric configuration. The polarization curves generated will be used as boundary conditions in a finite element analysis. In this way potential, current, and corrosion rate distributions on galvanic couples of complex geometries will be determined, including the effects of seawater path resistance. The use of this finite element analysis technique will be verified by application to a moderately complex galvanic couple—a condenser tube with a tube sheet. This portion of the program is addressed in a separate report.

APPROACH

Conduct long-term potentiostatic and short-term potentiodynamic polarization studies of a variety of naval alloys, while simultaneously exposing bimetal and multimetal galvanic couples. Use the data from the polarization studies to predict the behavior of complex galvanic couples involving a complex geometry. Verify the

4

prediction with actual exposures. In future work, extend results by testing naval alloys at seawater velocities greater than zero.

MATERIALS

Six materials were chosen for the initial phase of this study: (1) 90-10 copper nickel (C70600); (2) Monel 400 (N04400); (3) Inconel 625 (N06625); (4) Navy M-bronze (C92200); (5) nickel-aluminum bronze (C95800); and (6) HY-80 steel. These materials were chosen to represent a wide range of material classes which are utilized in marine environments. The two bronzes were obtained as castings while the other material is employed in a wrought condition. Later, Titanium 50 (R50400); 70-30 copper-nickel (C71500); and an anode grade zinc (MIL-STD 18001) were introduced into the study. Specifications and compositions of these materials are given in Table 1. Corrosion samples were prepared by rough cutting blanks from the bars or plates supplied, milling to approximate dimensions, and grinding to final dimensions with a 32-RMS (120-grit) finish.

METHODS

POTENTIOSTATIC POLARIZATION AND GALVANIC COUPLES

The equipment for potentiostaic polarization has been described previously.[8] However, because of test problems which led to considerable scatter and information loss, some equipment and procedures were modified. Therefore, a summary of equipment is warranted.

Corrosion Test Cells

For the long-term exposures, three specimens of identical materials exposed at the same potential for different lengths of time, were connected to the same potentiostat. In this way, all 30-, 60-, and 120-day exposures were conducted simultaneously. A series of individual exposure vessels was used to avoid ground loops between potentiostats or stray current effects in galvanic couple exposures. A total of 108 exposure vessels (rubber containers of abour 4-liter capacity) were fitted into two wooden boxes lined with thermal insulation. Heated, filtered, natural seawater was drip-fed into each container to maintain oxygen levels in the bulk solution at saturation and temperatures of 30°C. Quiescent flow conditions were maintained via the low refreshment rate. Corrosion coupons were suspended in

5

TABLE 1 - SPECIFICATIONS AND NOMINAL COMPOSITION OF MATERIALS TESTED

Material	SAE/ASTM UNS Number	Purchase Specification	Chemical Composition, wt%														
			Cu	Ni	Fe	C	Mn	P	S	Al	Zn	Ti	Sn	Pb	Mo	Si	Others
90-10 Cu-Ni	C70600	MIL-C-15726E	88.04	10.2	1.45	-	0.10	<0.02	<0.02	-	0.13	-	-	<0.2	-	-	-
Monel 400	N04400	QQ-N-281D	31.43	65.55	1.63	0.11	1.08	-	0.006	0.020	-	-	-	-	-	0.17	-
Inconel 625	N06625	ASTM-B443-75	-	62.15	3.46	0.02	0.16	0.013	-	0.15	-	0.26	-	-	8.41	0.25	21.46 Cr 3.66 Cb&Ta
M-Bronze	C92200	MIL-B-16541	86.91	0.45	0.09	-	-	-	-	-	4.74	-	6.05	1.7	-	-	0.06
Ni-Al Bronze	C95800	MIL-B-21230A	79.85	4.88	4.24	-	1.49	-	-	9.36	0.07	-	0.04	0.02	-	-	-
HY-80 Steel	-	MIL-S-16216H	0.046	2.83	Bal	0.15	0.23	0.012	0.020	-	-	0.001	-	-	0.47	0.27	<0.001 V 1.61 Cr
Titanium 50	R50400	MIL-T-7993	-	0.1	0.3	0.10	-	-	-	-	-	Bal	-	-	-	-	0.250 O_2
70-30 Cu-Ni	CA71500	-	68.02	30.34	0.60	<0.03	0.77	0.01	0.006	-	0.09	-	-	0.01	-	-	-
Anode Grade Zinc*	-	MIL-STD-18001	0.05 max	-	0.05 max	-	-	-	-	0.1-0.5	Bal	-	-	0.06 max	-	0.125 max	0.025 Cd max

*ZHS Anode Stock.

the exposure vessels by means of a threaded rod screwed into a hole tapped in the specimen edge. This rod was also used for electrical contact to the specimen. Water was excluded from the electrical-contact-mounting area by means of a glass tube and Teflon gasket. Platinum-coated counter electrodes were placed adjacent to specimen faces. Ag-AgCl reference electrodes were placed in the plane of the corrosion coupons directly below the specimens.

Some of the exposure vessels contained galvanic couples consisting of three specimens of each material so that sequential (30-, 60-, and 120-day) removals could be made. These vessels also contained Ag-AgCl reference electrodes but counter electrodes were not required. Other vessels contained three identical freely corroding specimens of each material for sequential removal at 30, 60, and 120 days. These exposure vessels also contained Ag-AgCl reference electrodes but no counter electrodes.

Instrumentation

A bank of 70 potentiostats constructed for this experiment were located in an adjacent, temperature-controlled room and were connected to 70 of the test cells through insulated electrical leads. Potential and current readings were taken by a computerized Data Acquisition System (DAS) described previously.[8] For the potentiostats employed, a 5 mV variation in set potential was maintained. A thermal instability coefficient of approximately 1 mV/°C (air temperature) and IR drop through cabling from the cell to the module were identified as the source of these variations. Electrical leads from the anode and cathode coupon groups (group of three) of each galvanic couple were connected in series to 1-ohm resistors. The potential drop across the 1-ohm resistors was then recorded by the DAS. For multimetal galvanic couples (3 alloys) each group (3 specimens) of alloys was connected in series to the other alloy groups through 1-ohm resistors. The extra 1 ohm of resistance has been found to insignificantly affect couple behavior in these tests.[8]

Experimental Procedure

For each material in potentiostatic polarization experiments, 15 to 17 potentials were chosen. The bimetal galvanic couples had a 1:1 ratio, while the multimetal couples had an area ratio of 1:1:1. The material combinations for couples and controls are listed in Table 2. Exposures were conducted simultaneously for all types of tests over the 120-day period.

7

Table 2
GALVANIC COUPLE COMBINATIONS AND CONTROLS

Bimetal Galvanic Couple Combinations

HY-80 coupled to Zinc

Ni-Al Bronze coupled to Zinc

90-10 Copper-Nickel to Zinc

Titanium 50 to Monel

Titanium 50 coupled to 70-30 Copper-Nickel

Monel coupled to 70-30 Copper Nickel

Inconel 625 coupled to 70-30 Copper Nickel

Inconel 625 coupled to Ni-Al Bronze

M-Bronze coupled to 70-30 Copper Nickel

M-Bronze coupled to 90-10 Cu-Ni

Multimetal (3) Galvanic Couple Combinations

HY-80 coupled to Ni-Al-Bronze coupled to Zinc

Ti-50 coupled to Inconel 625 coupled to 70-30 Copper-Nickel

Ti-50 coupled to 70-30 Copper-Nickel coupled to Zinc

Monel coupled to 90-10 Copper Nickel coupled to Zinc

Inconel 625 coupled to Ni-Al-Bronze coupled to Zinc

Inconel 625 coupled to Monel coupled to 70-30 Copper-Nickel

Monel coupled to Ti-50 coupled to Ni-Al-Bronze

Inconel 625 coupled to Ni-Al-Bronze coupled to 70-30 Copper Nickel

Freely Corroding Coupons (Controls)

HY-80	Inconel 625
Ni-Al-Bronze	Monel
M-Bronze	Anode Zinc
90-10 Copper Nickel	70-30 Copper Nickel
Titanium 50	

Data Acquisition

Currents, potentials, and temperatures were monitored and recorded automatically using the DAS. Current and potential data for constant potential specimens, galvanic couples, and freely corroding specimens were taken once per minute for the first day of exposure, every 10 minutes for the first week, and 3 times per day thereafter. From the initial 5-minutes and 1-day behavior of 30-, 60-, and 120-day runs, 5 minute and 1-day data was taken. There was no weight loss for 5-minute and 1-day measurements. Raw data was manipulated as follows:

Time Interval	Measurement Frequency	Manipulation
0 to 5 minutes	1/minute	none
5 minutes to 1440 minutes (1 day)	1/10 minutes	average* 1/30 minutes
1 day to 7 days	1/10 minutes	average to* 1/6 hours
7 days to 120 days	3 days	average to* 1/2 days

*Simple average not weighed.

Current data was normalized with respect to wetted surface area. Alarm limits for constant potential tests were set at ±7 mV.

For weight loss determinations, ASTM recommended procedures for cleaning, drying, and weighing were followed.[11] Special care was taken to make sure that the threaded hole was dry prior to weighing. Weight loss accuracy to 0.1 mg was achieved. Upon specimen removal surfaces were inspected, and representative photographs were taken.

POTENTIODYNAMIC POLARIZATION
Corrosion Test Cells and Instrumentation

Exposure vessels and coupon mounting were the same as for the potentiostatic exposures. Platinum-coated counter electrodes and a saturated Calomel reference electrode with luggin probe were utilized.

Instrumentation consisted of a PAR EG&G Model 173 potentiostat with a log current converter. Linear voltage-time ramps were provided using a PAR EG&G 175 programmer. Potential and current outputs were connected to an X-Y recorder for hardcopy and an Apple minicomputer via an analog-to-digital interface for data storage and retrieval.

Experimental Procedure

Specimens were studied under two conditions: 1-hour pre-exposure at open circuit potential in natural seawater and a 120-day pre-exposure under identical conditions. Generally, procedures followed ASTM standard G5-75 for Potentiodynamic Polarization Techniques.[12] Separate specimens were independently polarized anodically and cathodically starting at E_{corr}. Duplicate specimens were polarized at most scan rates. The four scan rates utilized are listed below:

Scan Rates

volt/hour	mV/sec
0.5	0.14
5	1.4
50	14
100	28

DATA ANALYSIS

POTENTIOSTATIC POLARIZATION AND GALVANIC COUPLE TESTS

Potentials

Potential-versus-time data for the potentiostatic test was utilized only to look for problems which would invalidata data from that exposure. Minor variations of ±5 mV in potentiostatic test potential were observed. Where such shifts occurred, the nominal potential was replaced with the actual values recorded at 5 minutes and 1, 30, 60 and 120 days for the final data analysis. Potentials for the long-term freely-corroding specimens, bimetallic, and multimetal couples were picked off of the potential-versus-time curves at 30, 60, and 120 days. Where duplicate exposures existed a composite curve was first constructed. Potential resolution

was limited by graphing accuracy to ±10 mV. This was reasonable, considering the data scatter and reproducibility where replicate data existed.

POTENTIOSTATIC CURRENTS

To obtain current densities, the current-versus-time plots for the long-term exposures were hand-fitted with smooth curves, values picked off at 30, 60, and 120 days, and these currents normalized with respect to wetted surface area for the number of specimens in test at that time. As with the potential data, where duplicate exposures existed, a composite curve was used. Current resolution for all exposures was limited to 0.2-0.6 $\mu A/cm^2$, depending on the number of specimens in test. Scatter was such that values below 0.2 $\mu A/cm^2$ were indistinguishable from zero. Potentiostatic current data for alloys not previously reported[8] is listed in Table 3.

Galvanic Couple Currents

To obtain current densities, the current-versus-time data was initially hand-fitted with smooth curves and values picked off at 30, 60, and 120 days. This procedure was found in some cases to be inaccurate due to rapid fluctuations in couple currents, including relative anode-cathode relationship reversals for some couples. For this reason, current-versus-time data was numerically integrated to yield a total value for the net anodic charge passed after 30-, 60-, and 120-day intervals. An average current density was then determined for the first 30 days of exposure, the following 30 days of exposure, and the remaining 60 days.

Weight Loss

Weight loss data for potentiostatic specimens not previously reported is shown in Table 4. Weight loss data for Inconel 625; Monel 400; M-bronze; 90-10 copper nickel; HY-80 steel; and nickel aluminum bronze is reported in reference 8. For anode grade zinc weight loss data is reported for 1-, 30-, 60-, and 120-day potentiostatic specimens; for 70-30 copper nickel and Ti-50, the 1-day weight loss is not reported due to its low value. Weight losses for Ti-50 are generally less than 1 mg at all potentials. Weight losses for bimetal and multimetal couples are reported for 30, 60, and 120 days for all anode materials. These weight losses are listed in Tables 5 and 6.

TABLE 3 – CURRENT DENSITIES FOR POTENTIOSTATIC
POLARIZATION SPECIMENS

Potential (mv) versus Ag/AgCl	Exposure Time				
	5 Minute ($\mu A/cm^2$)	1 Day ($\mu A/cm^2$)	30 Day ($\mu A/cm^2$)	60 Day ($\mu A/cm^2$)	120 Day ($\mu A/cm^2$)
70-30 Copper-Nickel					
99	1561	408	114	–	–
50	–	–	364	150	–
45	1900	916	–	–	–
0	1174	652	230	138	–
-50	–	–	–	–	238
-53	826	488	225	394	–
-100	825	74	3	2	7
-150	15	0.7	-0.3	0.3	2.2
-200	-4	-0.5	-7	-9	-15
-252	-11	-7.9	-10.0	-14.0	-23.0
-302	-17.5	-8.1	-8.5	-19.0	-20.0
-399	-21.0	-19.6	–	-19.5	-12.0
-402	–	–	-8.0	–	–
-500	-24.4	-27.0	-11.0	-11.0	-9.0
-600	-42.0	-39.0	-11.5	-18.5	-11.0
-700	-20.0	-36.5	-14.5	-23.0	-8.5
-800	-26.9	-13.5	-13.0	-26.0	-10.5
-1003	-49.0	-13.0	-15.0	-10.0	-9.0
E_{corr}(mV)	-188	-180	-134	-195	-195
Anode Grade Zinc (Mil-Spec 18001)					
-498	–	17,125	–	–	–
-513	22,500	–	–	–	–
-560	18,450	16,375	..	–	–
-600	17,000	15,000	–	–	–
-650	15,000	12,000	–	–	–
-700	14,500	11,960	–	–	–
-751	12,425	11,000	–	–	–
-800	10,000	8,750	–	–	–

TABLE 3 (Continued)

Potential (mV) versus Ag/AgCl	Exposure Time				
	5 Minute ($\mu A/cm^2$)	1 Day ($\mu A/cm^2$)	30 Day ($\mu A/cm^2$)	60 Day ($\mu A/cm^2$)	120 Day ($\mu A/cm^2$)
	Anode Grade Zinc (continued)				
-851	8,050	7,200	-	-	-
-895	-	4,025			
-904	6,225	-	-	-	-
-954	2,725	2,740	820		
-1000	1,150	1,260	490	345	200
-1050	17.7	20.0	-17.0	-10.5	-8
-1100	-17.6	-11.0	-16.0	-10.0	-6
-1150	-	-51.5	-20	-14.0	-9
E_{corr}(mV)	-1066	-1066	-1036	-1029	-1010
	Titanium 50				
200	1.05	0.1	0.2	0.4	0.9
152	0.75	-	-0.1	-0.1	0.3
145	-	0.14	-	-	-
98	0.7	0.16	-2.0	-0.45	-0.2
50	0.47	0.19	-	-0.01	-0.5
48	-	-	-3.3	-	-
0	1.15	0.2	-2.3	-0.6	-0.01
-50	0.26	0.2	-1.5	-0.1	-0.1
-98	0.01	0.16	-2.0	-0.5	-0.2
-146	0.3	-0.13	-5.0	-2.4	-0.1
-203	0.1	-0.14	-10.0	-20.0	-8.0
-248	-0.39	-0.35	-13.0	-22.5	-12.0
-301	-0.32	-0.65	-16.5	-15.0	-8.5
-400	-0.33	-7.5	-16.0	-14.0	-6.0
-600	-20.5	-35.5	-10.0	-9.0	-12.0
-800	-31.5	-33.0	-8.5	-13.5	-10.0
-1000	-64.0	-53.0	-20.0	-	-

TABLE 4 — WEIGHT LOSS FOR POTENTIOSTATIC POLARIZATION SPECIMENS

Potential (mV) versus Ag/AgCl	Exposure Time		
	30 Day (g)	60 Day (g)	120 Day (g)
.70-30 Copper Nickel (CA 715)			
99	14.0263	—	—
50	20.6221	32.9857	—
0	13.075	22.9491	—
-50	—	—	29.2810
-53	7.0282	15.6734	—
-100	0.2491	0.2929	0.5295
-150	0.0287	0.1215	0.0345
-200	0.0202	0.0158	0.0176
-252	0.0155	0.0188	0.0167
-302	0.0156	0.0184	0.0100
-399	—	0.0294	0.0118
-402	0.0127	—	—
-500	0.0127	0.0104	0.0056
-600	0.0079	0.0075	0.0106
-700	0.0087	0.0106	0.0060
-800	0.0091	0.0348	0.0108
-1003	0.0122	0.0019	0.0022
(Controls)	0.0245	0.0275	0.0316

TABLE 4 (Continued)

Potential (mV) versus Ag/AgCl	Exposure Time		
	30 Day (gm)	60 Day (gm)	120 Day (gm)
	Titanium 50		
200	0.0010	0.0020	0.0005
152	0.0015	0.0011	0.0014
98	0.0005	0.0031	0.0017
50	–	0.0019	0.0017
48	0.0014	–	–
0	0.0007	0.0006	0.0007
-50	0.0013	0.0014	0.0010
-98	0.0006	0.0022	0.0008
-146	0.0006	0.0011	0.0010
-203	0.0004	0.0010	0.0015
-248	0.0005	0.0010	0.0007
-301	0.0009	0.0010	0.0015
-400	0.0007	0.0023	0.0003
-600	0.0014	0.0007	0.0001
-800	0.0006	0.0008	0.0001
-1000	0.0002	0.0017	0.0009
Controls	0.0001	0.0017	0.0009

TABLE 4 (Continued)

Potential (mV) versus Ag/AgCl	Exposure Time			
	1 Day (g)	30 Day (g)	60 Day (g)	120 Day (g)
Anode Grade Zinc				
-498	14.9362	-	-	-
-513	-	-	-	-
-560	13.4955	-	-	-
-600	12.7584	-	-	-
-650	10.4132	-	-	-
-700	9.7684	-	-	-
-751	7.9115	-	-	-
-800	6.4261	-	-	-
-851	5.9117	-	-	-
-895	4.7184	-	-	-
-904	-	26.8316	-	-
-954	-	12.5573	57.6469	-
-1000	-	12.2231	23.3720	34.2880
-1050	-	0.0866	0.1288	0.1155
-1100	-	0.0132	0.0141	0.0088
-1150	-	0.0159	0.0202	0.0075
(Controls)	-	0.2581	0.3929	0.2082

16

TABLE 5 - WEIGHT LOSS FOR BIMETAL GALVANIC COUPLE SPECIMENS

Material		Exposure Duration (days)	Anode Weight Loss (g)	Control Weight Loss (g)
Cathode	Anode			
HY-80	Zinc	30	0.1802	0.2581
		60	0.4459	0.3929
		120	0.7091	0.2082
Ni-Al-Bronze	Zinc	30	0.1935	0.2581
		60	0.4453	0.3929
		120	0.7153	0.2082
90-10 Cu-Ni	Zinc	30	0.1730	0.2581
		60	0.4883	0.3929
		120	0.8322	0.2082
Titanium 50	Monel 400	30	0.1043	0.0988
		60	0.1002	0.0949
		120	0.1978	0.0384
Monel 400	70-30 Cu-Ni	30	0.0574	0.0245
		60	0.0887	0.0275
		120	0.2910	0.0316
Inconel 625	70-30 Cu-Ni	30	0.0836	0.0245
		60	0.2291	0.0275
		120	0.5135	0.0316
Inconel 625	Ni-Al-Bronze	30	0.2446	0.2446
		60	0.1948	0.1948
		120	0.2773	0.2773
90-10 Cu-Ni	M-Bronze	30	0.0764	0.0820
		60	0.1174	0.1118
		120	0.1577	0.1658
Titanium 50	70-30 Cu-Ni	30	0.0742	0.0245
		60	0.0949	0.0275
		120	0.2090	0.0316

TABLE 6 – WEIGHT LOSS FOR MULTIMETAL GALVANIC COUPLE SPECIMENS

Materials	Cathode Materials	Anode Materials	Exposure Duration (days)	Anode Weight Loss (g)	Control Weight Loss (Anode Material) (g)
Ni-Al-Bronze HY-80 Steel Anode Zinc	Ni-Al-Bronze HY-80 Steel	Anode Zinc	30 60 120	0.5322 0.7844 1.1355	0.2581 0.3929 0.2082
Titanium 50 Inconel 625 70-30 Cu-Ni	Titanium 50 Inconel 625	70-30 Cu-Ni	30 60 120	0.1300 0.3588 0.6125	0.0245 0.0275 0.0316
Titanium 50 70-30 Cu-Ni Anode Zinc	Titanium 50 70-30 Cu-Ni	Anode Zinc	30 60 120	0.3762 0.6506 1.3211	0.2581 0.3929 0.2082
Monel 400 90-10 Cu-Ni Anode Zinc	Monel 400 90-10 Cu-Ni	Anode Zinc	30 60 120	0.2923 0.3147 0.5711	0.2581 0.3929 0.2082
Inconel 625 Ni-Al-Bronze Anode Zinc	Inconel 625 Ni-Al-Bronze	Anode Zinc	30 60 120	0.4460 0.8821 1.7652	0.2581 0.3929 0.2082
Inconel 625 Monel 400 70-30 Cu-Ni	Inconel 625 Monel 400	70-30 Cu-Ni	30 60 120	0.1980 0.2602 0.5712	0.0245 0.0275 0.0316
Titanium 50 Monel 400 Ni-Al-Bronze	Titanium 50 Monel 400	Ni-Al-Bronze	30 60 120	0.0404 0.1123 0.5284	0.0460 0.0291 0.1009
Inconel 625 Ni-Al-Bronze 70-30-Cu-Ni	Inconel 625	Ni-Al-Bronze	30 60 120	0.0568 0.1453 0.4849	0.0460 0.0291 0.1009
		70-30 Cu-Ni	30 60 120	0.0225 0.0306 0.0311	0.0245 0.0275 0.0316

Visual Appearance

Observations were made on specimen appearance at 30-, 60-, and 120-day removal dates for specimens potentiostatically polarized, freely corroding controls, and galvanic couples. Corrosion products and calcareous deposits were removed and stored for the possibility of energy dispersive X-ray analysis and X-ray diffraction analysis for compositional and compound identification, respectively. The visual observations are discussed in the "Summary of Observations" section which appears in the appendix. It is useful to point out that corrosion products on anodically polarized specimens visually appeared similar to those observed on galvanic couple anodes in many instances.

RESULTS AND DISCUSSION

POTENTIOSTATIC POLARIZATION

The current data from the constant potential exposures is plotted as a function of potential (E) in Figures 1 through 9. Figures 1 through 6 were reported previously but are included for comparison to potentiodynamic data.[8]

The open circuit potentials of Ti-50, anode zinc, and 70-30 copper-nickel drifted with time, as reported for the other six materials.[8] The most extreme examples of this were the Ti-50 and the Inconel 625. For the titanium the corrosion potential drifted from -130 to +195 mV over the first 30 days. It never stabilized and dropped to as low as -100 mV several times during the remainder of the 120-day immersion. Large potential drifts had been noted previously for Inconel 625. Apparently, with regard to potential variations, the oxide film is not stable under these low-velocity conditions. Ni-Al-bronze drifted almost 200 mV positive and stabilized by the 30th day. Zinc anode material drifted slightly with time, from -1100 to -1025 mV after the first 10 days, where the potential remained relatively stable. During the 120-day immersion, both 70-30 and 90-10 copper nickel remained in the range of -100 to -200 mV, remaining stabilized after 30 days. Bronze composition M did not exhibit any drift in its open-circuit potential. HY-80 steel experienced a rapid negative shift of over 100 mV which stabilized by the end of the first day.

Many practical galvanic couples exist where the two coupled materials are within a few hundred millivolts of each other. It is within this range that polarization currents are most affected by changes in open-circuit potential; thus the existence of the shift in this potential will cause significant time effects on galvanic currents on couples between materials with potentials that are close.

19

Except for Monel 400, the anodic current densities of all materials tended to decrease with time, possibly due to the buildup of corrosion products serving as barrier films to ionic migration. In some materials, current decreases could also be due to the lowering of the anodic overvoltage due to the positive drift of the corrosion potential. Inconel 625 and titanium 50 showed only slight, if not negligible, anodic currents, considering the degree of accuracy of the experimental methods.

At about 0 mV, 70-30 copper-nickel exhibited an area of either resistive film buildup or passivity. The decrease in current at potentials in this region became more pronounced as exposure duration increased. Similar behavior was noted for 90-10 copper-nickel in the previous experiments. This passivity is likely caused by a change in corrosion product structure or composition, or a valence change of copper in the corrosion products, i.e. $Cu_2O \rightarrow CuO$. The mere presence of an adherent corrosion product acting as a barrier to ionic migration could cause similar behavior. Ohmic contributions cannot be ruled out; however, their contribution does not entirely explain the observed behavior.

Although data scatter is large, cathodic current densities tended to decrease with exposure duration (up to 30 days duration) after which the currents were constant at all potentials except those more negative than -1000 mV. This is consistent with earlier work. For all alloys tested strict oxygen diffusion-control prevails below -300 mV. Calcareous product formation (i.e. $CaCO_3$, $Mg(OH)$)[13] was observed on cathodically polarized samples, and such formations occluded surface area, thereby contributing to reduction of current density with time. Presumably, the calcareous deposition covers enough surface area to minimize the current contributions from hydrogen reduction, occurring at -800 mV and more electronegative potentials. The cathodic curves for all materials after 30 days of exposure tended to be flat and to scatter within the same range, 6 to 20 $\mu A/cm^2$. This behavior implies that the cathodic kinetics for all nine materials were similar after 30 days for the specific flow conditions described. This indicates an oxygen-diffusion-controlled mechanism, as might be expected from the low seawater flow rate involved. Increase in flow should increase the value of this "plateau" as mass transport of oxygen to the metal/electrolyte interface is promoted. Since all materials had similar limiting values of cathodic current, all should behave similarly in a galvanic couple where the couple potential is significantly more cathodic than the open-circuit potential of these materials under the

20

conditions specified. For example, nearly all of these materials (except zinc) should, under quiescent conditions, cause nearly the same current demand on a zinc cathodic protection system designed to protect at potentials below -750 mV.

WEIGHT LOSS FROM CONSTANT POTENTIAL EXPOSURES

Weight loss data has been used to derive corrosion rate versus potential curves as the examples in Figures 10 and 11 illustrate. All data for Ti-50 is below 3×10^{-3} mm/yr; therefore, this plot is excluded. For the 70-30 copper-nickel and zinc anode material, corrosion rates decrease very slightly with time at anodic potentials and decrease by one order of magnitude over the 120-day period at cathodic overpotentials. Corrosion rate versus potential plots for Inconel 625, HY-80 steel, 90-10 copper-nickel, M-bronze, nickel aluminum bronze, and Monel 400 are shown in Reference 8. A good correlation between corrosion rate and measured anodic current is obtained.

POTENTIODYNAMIC POLARIZATION

The anodic and cathodic potential scans are plotted in Figures 12-23. Data from the anodic and cathodic potential scans with 1 hour pre-exposure are plotted in Figures 12 through 17; data from specimens with 120-day pre-exposure are plotted in Figures 18 through 23. The data presented has not been IR corrected. IR compensation generally had a significant effect at current densities greater than 10^3 $\mu A/cm^2$ for the existing cell parameters. In specimens pre-exposed for 1 hour, there was little effect of scan rate on the anodic curves except in passive regions, including the region around 0 mV on the three copper-based alloys, the region at -250 mV on nickel-aluminum bronze, and at -100 mV on Monel 400. Some degree of passivation, or at least a decrease of anodic current, was observed in these potential regions. In all cases better resolution was achieved in passivation areas when low scan rates were utilized. The entire anodic curve for Inconel 625 also fell into this category, since this material is in a region of strong passivity even at its open-circuit potential.

Specimens pre-exposed for 120 days had more complex effects of scan rate on the anodic curves. Inconel 625 and 90-10 copper-nickel had anodic currents that decreased at a given overpotential with decreasing scan rate. Monel 400 experienced no resolvable effect of scan rate, and the other three alloys experienced nonsystematic effects of scan rate on anodic current densities.

21

Anodic current densities for the long-term potentiostatic curves were usually much better matched by potentiodynamic data from specimens pre-exposed for 120 days than from those pre-exposed for only 1 hour. The bronze alloys had a close match between long-term potentiostatic and 120-day pre-exposed potentiodynamic anodic curves for potentials within 40 mV of the open-circuit potential. Monel 400 curves matched for potentials within 100 mV of the corrosion potential, while HY-80 matched for 150 mV. Inconel 625 experienced such low anodic currents that lack of match between curves was relatively insignificant. The lack of reproducibility of open-circuit potentials prevented any good matching for 90-10 copper-nickel. Anodic Tafel slopes were measured from IR corrected potentiodynamic polarization curves. Values for all six materials ranged from 60 to 450 mV/decade, with values of 100-200 being typical. There was no systematic effect of scan rate on these values. However, with regard to pre-exposure, Tafel slopes for 120-day specimens fell in the high end of the 60 to 450 mV/decade range while Tafel slopes for 1 hour pre-exposures were in the low end. For comparison, Tafel slopes from long-term potentiostatic data for all materials except Inconel 625 were much lower (30-40 mV/ decade).

In summary, anodic long-term potentiostatic polarization data could best be approximated using low-scan rate potentiodynamic data on specimens pre-exposed for 120 days.

Cathodic curves tended towards the vertical at negative potentials, indicating the onset of diffusion control. In almost all cases, lower currents were observed at lower scan rates, probably due to the increase of the diffusion layer thickness for dissolved oxygen occurring during the longer scans. Currents were generally an order of magnitude higher than those from long-term potentiostatic tests, indicating that a steady-state diffusion layer thickness had not been reached during even the lowest scan. Presumably, a higher seawater flow rate would lead to a more rapid establishment of a lower steady-state diffusion layer thickness. This would result in higher but, nevertheless, steady-state currents. There was little difference in cathodic current between specimens pre-exposed for 1 hour and for 120 days for all alloys with one exception; 90-10 copper-nickel had a significantly lower cathodic current density if pre-exposed for 120 days. This agrees with observations that the Cu_2O corrosion product film is a poor substrate for the oxygen reduction reaction.[14]

In summary, cathodic potentiodynamic data could not be obtained which would approximate cathodic data from long-term potentiostatic tests.

PREDICTION OF BIMETALLIC GALVANIC CORROSION USING POTENTIODYNAMIC POLARIZATION

Actual bimetallic galvanic couple results from previous exposures and current work, along with predicted results from this potentiodynamic data are shown in Tables 7 and 8. Since duplicate polarization curves were generated, the average of four possible galvanic current densities is reported for each prediction shown. For 120-day pre-exposed specimens, potentiodynamic polarization data was useful in predicting galvanic couple currents and potentials, since the low scan rate polarization curves (0.14 and 1.4 mV/sec) yielded some agreement with long-term potentiostatic data. In some instances agreement is better with 0.14 mV/sec scan rate results; in other cases, agreement is better with 1.4 mV/sec data. Agreement within 20% was observed, and discrepancies by a factor of 2 were commonplace. Log-log extrapolation of galvanic current data at various scan rates to low scan rates improved results slightly in some instances. The fast scans of 5 V/hour to 100 V/hour were found to drastically overestimate galvanic current.

For 1-hour pre-exposed specimens, potentiodynamic polarization data also demontrated some utility in predicting galvanic couple currents and potentials. For Inconel 625/HY-80 steel, a galvanic current within 20% of the actual value at 120 days is predicted successfully. For Ni-Al-bronze/HY-80 and Monel 400/Inconel 625, extrapolation to a low scan rate is required to give accurate predictions of 30-day results, and no accurate prediction of 120-day results appears feasible. For both 120-day and 1-hour pre-exposed specimens, galvanic couple potentials may be in error by as much as 100 mV.

With regard to utilization of potentiodynamic polarization data for galvanic corrosion prediction, some utility has been demonstrated, although it is difficult to determine "a priori" which technique (i.e. slow scan rate or extrapolation to very low scan rate) is appropriate. Marginally better data is obtained from 120-day pre-exposures than 1-hour pre-exposures.

TABLE 7 – COMPARISON OF PREDICTED AND ACTUAL GALVANIC COUPLE PARAMETERS
(from 120-Day Pre-Exposed Potentiodynamic Data)

Material		Expo-sure Dura-tion (days)	Actual (Measured) Current Density* (µA/cm²)	Predicted Current Density (µA/cm²)					Couple Potential (mV) versus Ag/AgCl	
Anode	Cathode			Extrapolation to Zero Scan Rate	Scan Rate** (mV/s)				Actual	Predicted
					0.14	1.4	14.0	28		
H-80 Steel	Ni-Al-Bronze	30	23						-630 to -680	-480 to -630
		60	11	19***	39	47	120	105		
		120	4.8							
90-10 Cu-Ni	Monel 400	30	1.4						-110 to -140	-200 to -300
		60	4.8	–	0.6	10	18	32		
		120	3.4							
Monel 400	Inconel 625	30	7.9						-40	-30 to -80
		60	5.7	–	<0.1	2.6	2.7	5.5		
		120	0.02							
Ni-Al-Bronze	Monel 400	30	9.5						-160 to -200	-150 to -250
		60	5.0	2.7***	5	6.6	14.4	17.0		
		120	11.0							
HY-80 Steel	Inconel 625	30	7.6						-640 to -680	-550 to -650
		60	7.8	4***	8	9	35	60		
		120	9.0							
Ni-Al-Bronze	Inconel 625	30	4.8						-145 to -160	-120 to -220
		60	1.2	–	<0.1	3	7	15		
		120	10							
M-Bronze	90-10 Cu-Ni	30	<0.1						-116 to -145	-210 to -280
		60	0.1		<0.1	13	11	6.3		
		120	0.2							

*1-ohm resistor data.
**Average of four possible couple current densities.
***log-log extrapolation.

TABLE 8 - COMPARISON OF PREDICTED AND ACTUAL
GALVANIC COUPLE PARAMETERS
(from 1-Hour Pre-Exposed Potentiodynamic Data)

| Material | | Expo-sure Dura-tion (days) | Actual (Measured) Current Density* ($\mu A/cm^2$) | Predicted Current Density ($\mu A/cm^2$) Extrapolation to Zero Scan Rate | Scan Rate** (mV/s) | | | | Couple Potential (mV) versus Ag/AgCl | |
Anode	Cathode				0.14	1.4	14.0	28	Actual	Predicted
HY-80 Steel	Ni-Al Bronze	30 60 120	23 11 4.8	20***	40	45	100	125	-630 to -680	-575 to -595
90-10 Cu-Ni	Monel 400	30 60 120	1.4 4.8 3.4	-	±2	±2	±2	±1	-110 to -140	-170 to -218
Monel 400	Inconel 625	30 60 120	7.9 5.7 0.02	7***	12	13	18	30	-130 to -150	-200
Ni-Al-Bronze	Monel 400	30 60 120	9.5 5.0 11.0	-	10	9	8	10	-315 to -350	-160 to -200
HY-80 Steel	Inconel 625	30 60 120	7.6 7.8 9.0	4***	8	13	25	35	-640 to -680	-575 to -630
Ni-Al-Bronze	Inconel 625	30 60 120	4.8 1.2 10	-	1.2	1.5	2.7	5	-145 to -250	-120 to -200
M-Bronze	90-10 Cu-Ni	30 60 120	<0.1 0.1 0.2	-	<0.1	<0.1	<0.1	<0.1	-116 to -145	-210 to -240

*1 ohm resistor data.
**Average of four possible couple current densities.
***log-log extrapolation.

BIMETALLIC GALVANIC COUPLE PREDICTIONS USING POTENTIOSTATIC POLARIZATION CURVES

Previous efforts demonstrated that predicted galvanic currents could be determined which were accurate within ±50% of the actual values in most cases[8] (as shown in Table 9). As an extension of the existing data base, additional galvanic bimetallic couple predictions were performed and are listed in Table 10. In most instances the actual values fell within ±50% of predicted values. The most accurate prediction was within ±5% of actual value. For the worst-case prediction, 200% error was present. In most instances, however, the actual values fell within ±50% of predicted values.

The actual couple potentials were always within 60 mV of those predicted, with the exception of couples involving Inconel 625 and Titanium 50. The problem with couples involving Titanium 50 and Inconel 625 could be associated with the erratic potential shifts noted for these alloys under quiescent exposure conditions.

Anode corrosion rates were predicted by cross-referencing the predicted couple potentials with corrosion rate versus potential curves. This is less accurate than other methods, since the result is a prediction based upon a prediction, resulting in compounded errors. Despite this, there was agreement between predicted and actual corrosion rates within a factor of 2 to 3 for most data.

MULTIMETAL GALVANIC COUPLE PREDICTIONS USING POTENTIOSTATIC POLARIZATION CURVES

Electrochemical principles applied to multimetal couples dictate that for the entire system the total rate of oxidation (sum of anodic currents) must equal the total rate of reduction (sum of cathodic currents) and, assuming no ohmic resistance, the entire system will reside at a single mixed potential. While an intermediate alloy in the multimetal couple may be anodic to one alloy and cathodic to another, its overall status as an anode or cathode can be determined if the algebriac sum of the two separate anodic and cathodic currents acting on the alloy is known. Essentially, five cases exist when a third alloy is introduced into a binary galvanic couple (assuming equal areas of all metals).[15] These cases are:

(1) The third material may be sufficiently noble to serve alone as the cathode, interacting with two anodes. In this study these circumstances result in a 1:2 cathodic/anode ratio.

TABLE 9 – COMPARISON OF PREDICTED AND ACTUAL GALVANIC COUPLE PARAMETERS
FROM LONG–TERM POTENTIOSTATIC DATA (Reference 8)

| Material | | Exposure Duration (days) | Current Density, μA/cm² | | Couple Potential mV versus Ag/AgCl | | Anode Corrosion Rate (mm/yr) | |
Anode	Cathode		Predicted	Actual*,**	Predicted	Actual	Predicted	Actual
HY-80 Steel	Ni-Al Bronze	30	9.8	23	-630	-680	0.45	0.25, 0.15
		60	8.1	1i	-635	-650	0.32	0.18, 0.32
		120	5.4	4.8	-640	-630	0.23	0.16, 0.24
90-10 Cu-Ni	Monel 400	30	6.0	1.4	-140	-110	1.2	0.04, 0.05
		60	7.8	4.8	-150	-120	1.1	0.13, 0.05
		120	7.0	3.4	-130	-140	2.0	0.03, 0.04
90-10 Cu-Ni	M-Bronze	30	0.16	0.02	-160	-150	0.03	0.02, 0.02
		60	0.16	0.02	-160	-150	0.02	0.01, 0.02
		120	0.16	0.02	-150	-130	0.02	0.01, 0.01
Monel 400	Inconel 625	30	0.16(12***)	7.9	-50	-40	0.06	0.09, 0.05
		60	0.16(6.2***)	5.7	-50	-40	0.05	0.09, 0.09
		120	0.16	0.02	-50	-40	0.02	0.08, 0.04
Ni-Al-Bronze	Monel 400	30	16	9.5	-150	-160	0.20	0.07, 0.17
		60	16	5.0	-150	-210	0.20	0.14, 0.16
		120	16	11	-150	-200	0.20	0.13, 0.09
HY-80 Steel	Inconel 625	30	9.6	7.6	-635	-680	0.32	0.15, 0.13
		60	9.3	7.8	-635	-660	0.32	0.19, 0.19
		120	6.5	9.0	-640	-640	0.23	0.17, 0.19

*Average of two couples with current monitored differently.
**1 ohm resistor and ZRA currents picked off at 30, 60, and 120 days.
***Based on anodic curve and observed couple potential.

27

TABLE 10 – COMPARISON OF PREDICTED AND ACTUAL GALVANIC COUPLE PARAMETERS: BIMETALLIC COUPLES

Material		Exposure Duration (days)	Current Density ($\mu A/cm^2$)		Couple Potential (mV) vs Ag/AgCl		Anode Corrosion Rate (mm/yr)	
Cathode	Anode		Predicted	Actual*	Predicted	Actual	Predicted	Actual
HY-80	Zinc	30	11.0	7.1	-1025	-1035	0.43	0.160
		60	9.0	9.4	-1025	-1032	0.43	0.198
		120	6.0	2.4	-1024	-1030	0.43	0.157
Ni-Al-Bronze	Zinc	30	10.5	4.3	-1025	-1021	0.43	0.172
		60	6.5	5.9	-1024	-1032	0.43	0.198
		120	2.0	5.1	-1023	-1036	0.43	0.159
90-10 Cu-Ni	Zinc	30	15.0	5.0	-1024	-1031	0.43	0.154
		60	10.0	10.1	-1023	-1031	0.43	0.217
		120	9.0	5.5	-1022	-1031	0.43	0.185
Titanium 50	Monel 400	30	1.8	1.4	- 70	- 55	0.045	0.075
		60	0.3	1.2	- 90	-130	0.022	0.036
		120	<0.2	<0.1	-130	- 95	-	0.035
Monel 400	70-30 Cu-Ni	30	3.0	1.1	-100	-125	0.180	0.041
		60	2.5	0.4	-102	-130	0.095	0.031
		120	4.2	1.7	-110	-110	0.070	0.052
Inconel 625	70-30 Cu-Ni	30	1.3	2.2	-101	-106	0.180	0.059
		60	1.9	1.0	-120	- 62	0.045	0.051
		120	2.0	3.5	-160	- 50	0.0085	0.127
Inconel 625	Ni-Al-Bronze	30	5.5	4.0	-145	-145	0.180	0.202
		60	4.5	3.5	-155	-250	0.180	0.081
		120	-	3.9	-	-	-	0.057
90-10 Cu-Ni	M-Bronze	30	0.3	0.2	-173	-116	0.150	0.057
		60	0.4	<0.1	-171	-115	0.170	<0.044
		120	-	0.2	-	-145	-	0.060
Titanium 50	70-30 Cu-Ni	30	2.1	1.0	-110	-121	0.150	0.053
		60	1.2	0.4	-120	-105	0.045	0.034
		120	0.5	1.1	-170	- 70	0.0080	0.037

*Based on coulombs of anodic charge passed during first 30, second 30, and final 60 days of experiments.

(2) The third material may act as a cathode, along with the original cathode in the binary system. These circumstances result in a 2:1 cathode/anode ratio.

(3) The third material may reside at the mixed potential of the original binary couple and corrode freely at its own open circuit potential without participating in the binary galvanic couple. These circumstances result in a 1:1 cathode/anode ratio between the original materials in the binary system.

(4) The third material may be anodic to one material and comparable to the anode in the original binary system, resulting in a 1:2 cathode/anode ratio.

(5) The third material may be anodic to both materials in the original binary couple, resulting in a 2:1 cathode to anode ratio.

To predict multimetal galvanic couple parameters for a given system involving three or more alloys, polarization curves for all alloys can be superimposed simultaneously. Total anodic and cathodic current at each potential can be determined algebrically, and a unique solution for couple potential and current can then be determined, as described by Tomashov.[15] Assumptions can be made based on polarization characteristics and open-circuit potentials as to which of the above mentioned cases was actually operative. For instance, in the zinc, HY-80, Ni-Al-bronze system, it is reasonable to assume both Ni-Al-bronze and HY-80 steel to be polarized sufficiently cathodic to be rendered cathodes, despite anodic behavior of steel with respect to Ni-Al-bronze in a binary system. As a preliminary step, superposition of binary systems was performed to aid in the determination of an approximate couple potential for all three materials simultaneously. This couple potential was checked to determine if anodic currents equalled cathodic currents; if not, the potential was adjusted accordingly. This resulted in an iterative process. Despite these and other complications, the predictive methods demonstrated some utility. The results are shown in Table 11. Most currents are within a factor of 2 or 3 of the predictions. Agreement as near as 10% and discrepancies by a factor of 10 were observed. As with the bimetal couples, the largest errors were associated with Monel 400 and, to a lesser extent, Titanium 50. Most multimetal couples studied fell in the category of 2:1 cathode to anode ratio. For the system Inconel 625, Monel 400, and 70-30 copper nickel, however, Monel 400 at open circuit resided nearly at the mixed couple potential between Inconel 625 and 70-30 copper-nickel, resulting in a system with a 1:1 cathode/anode ratio. Bimetallic data for

TABLE 11 – COMPARISON OF PREDICTED AND ACTUAL MULTIMETAL GALVANIC COUPLE CURRENTS FROM POTENTIOSTATIC DATA

Materials	Cathode	Anode	30 Day Net Anodic Current ($\mu A/cm^2$)		60 Day Net Anodic Current ($\mu A/cm^2$)		120 Day Net Anodic Current ($\mu A/cm^2$)	
			Predicted	Actual*	Predicted	Actual*	Predicted	Actual*
Ni-Al-Bronze HY-80 Steel Anode Zinc	Ni-Al-Bronze HY-80 Steel	Anode Zinc	17.4	7.6	11.7	4.3	4.8	4.9
Titanium 50 Inconel 625 70-30 Cu-Ni	Titanium 50 Inconel 625	70-30 Cu-Ni	2.9	2.2	2.0	1.2	2.0	3.0
Titanium 50 70-30 Cu-Ni Anode Zinc	Titanium 50 70-30 Cu-Ni	Anode Zinc	26.0	6.6	17.7	6.9	12.1	5.8
Monel 400 90-10 Cu-Ni Anode Zinc	Monel 400 90-10 Cu-Ni	Anode Zinc	30.5	4.6	21.5	1.9	8.1	2.3
Inconel 625 Ni-Al-Bronze Anode Zinc	Inconel 625 Ni-Al-Bronze	Anode Zinc	16.9	11.7	18.1	5.7	5.7	6.1
Inconel 625 Monel 400 70-30 Cu-Ni	Inconel 625 Monel 400	70-30 Cu-Ni	4.0	2.6	2.9	1.3	3.0	1.8
Titanium 50 Monel 400 Ni-Al-Bronze	Titanium 50 Monel 400	Ni-Al-Bronze	11.9	1.7	11.8	2.4	5.0	5.8
Inconel 625 Ni-Al-Bronze 70-30 Cu-Ni	Inconel 625	Ni-Al-Bronze 70-30 Cu-Ni	6.0 2.1	3.0 .1.6	4.5 1.2	0.7 3.6	2.0 0.5	0.9 4.5

*Based on coulombs of anodic charge passed during first 30, second 30, and final 60 days of experiments.

Inconel 625 and 70-30 copper nickel supports this. For the system Inconel 625, Ni-Al-bronze, and 70-30 copper nickel, a 1:2 cathode/anode ratio exists.

Multimetal couple potentials are listed in Table 12. In all but three cases, predicted multimetal couple potentials fell within 30 mV of actual values.

CONCLUSIONS

The behavior of bimetal galvanic couples as measured by galvanic current, couple potential, and corrosion rate of anode was predicted using both long-term potentiostatic polarization curves and short-term potentiodynamic polarization techniques. Although the best prediction capability utilizes long-term potentiostatic data, potentiodynamic data from 120-day pre-exposured, low scan rate tests has demonstrated some utility. In addition the galvanic behavior of multimetal systems consisting of three alloys was successfully predicted using potentiostatic data. Extension to multimetal systems containing four or more alloys is believed to be feasible. Galvanic couple parameters were predicted to levels of accuracy equivalent to, or greater than, the popular galvanic corrosion prediction techniques using galvanic corrosion rate tables or potential differences in a galvanic series.

ACKNOWLEDGMENTS

TABLE 12 – COMPARISON OF PREDICTED AND ACTUAL MULTIMETAL
GALVANIC COUPLE POTENTIALS FROM POTENTIOSTATIC DATA

Materials	Cathode	Anode	30 Day Couple Potential (mV) vs Ag/AgCl		60 Day Couple Potential (mV) vs Ag/AgCl		120 Day Couple Potential (mV) vs Ag/AgCl	
			Predicted	Actual	Predicted	Actual	Predicted	Actual
Ni-Al-Bronze HY-80 Steel Anode Zinc	Ni-Al-Bronze HY-80 Steel	Anode Zinc	-1003	-1030	-1002	-1010	-1006	-1020
Titanium 50 Inconel 625 70-30 Cu-Ni	Titanium 50 Inconel 625	70-30 Cu-Ni	-110	-100	-125	-117	-100	-40
Titanium 50 70-30 Cu-Ni Anode Zinc	Titanium 50 70-30 Cu-Ni	Anode Zinc	-1000	-1025	-1000	-1025	-1003	-1019
Monel 400 90-10 Cu-Ni Anode Zinc	Monel 400 90-10 Cu-Ni	Anode Zinc	-1000	-1030	-1001	-1010	-1003	-1020
Inconel 625 Ni-Al-Bronze Anode Zinc	Inconel 625 Ni-Al-Bronze	Anode Zinc	-1000	-1020	-1001	-1000	-1004	-1001
Inconel 625 Monel 400 70-30 Cu-Ni	Inconel 625 Monel 400	70-30 Cu-Ni	-95	-85	-95	-105	-105	-80
Titanium 50 Monel 400 Ni-Al-Bronze	Titanium 50 Monel 400	Ni-Al-Bronze	-156	-180	-157	-205	-165	-185
Inconel 625 Ni-Al-Bronze 70-30 Cu-Ni	Inconel 625	Ni-Al-Bronze 70-30 Cu-Ni	-150	-153	-155	-208	-160	-185

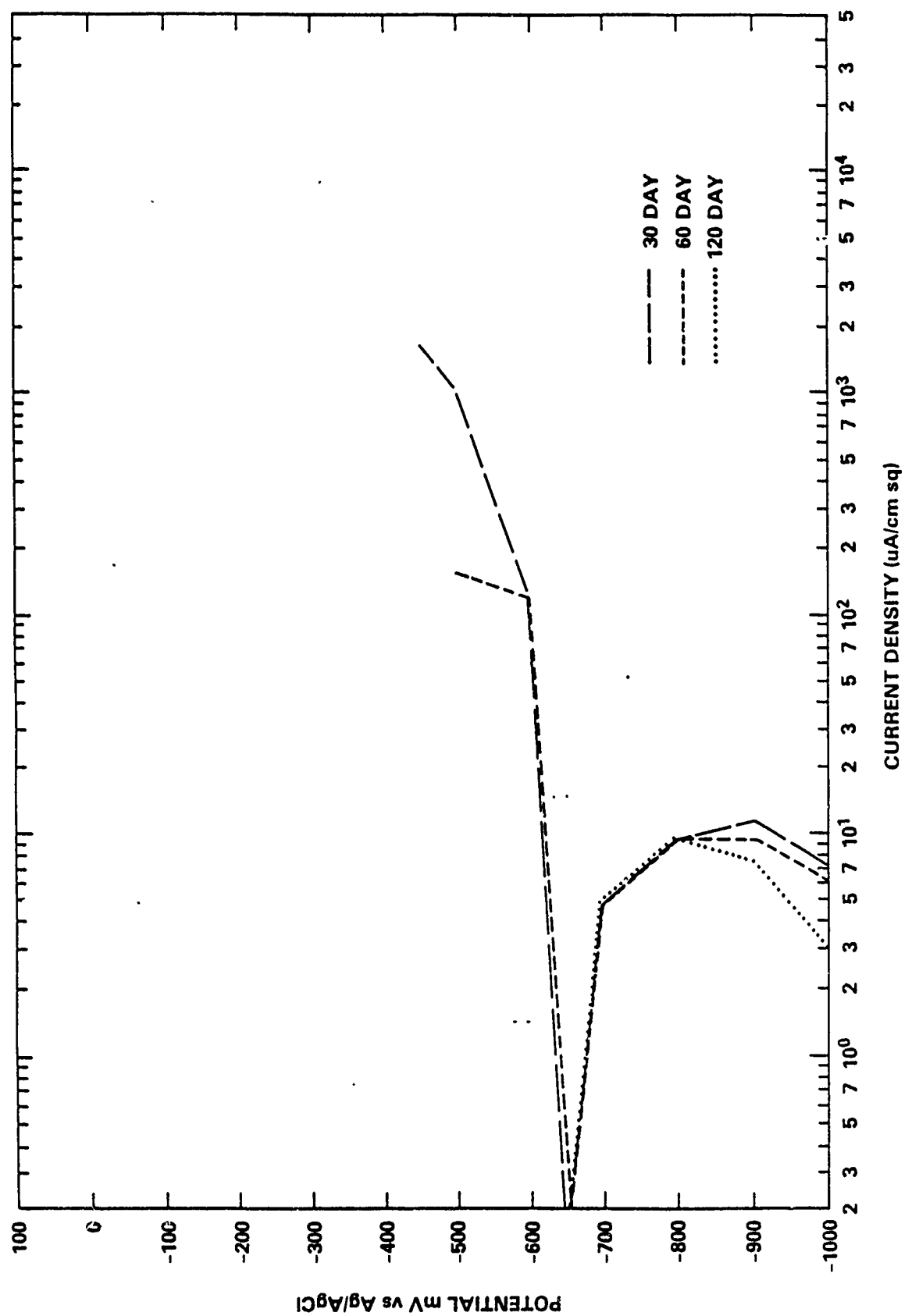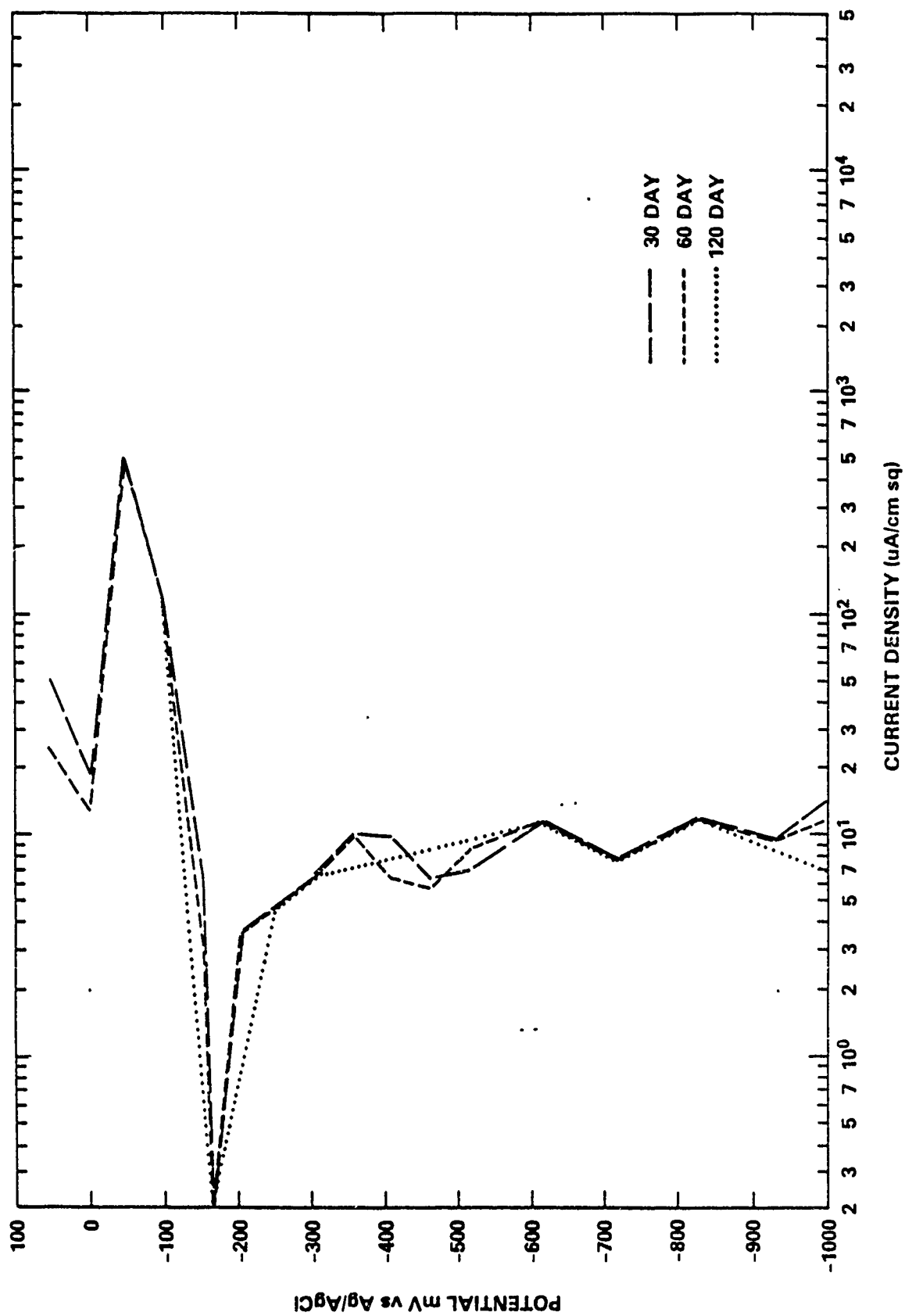Figure 1 – Potentiostatic Polarization of HY-80 Steel

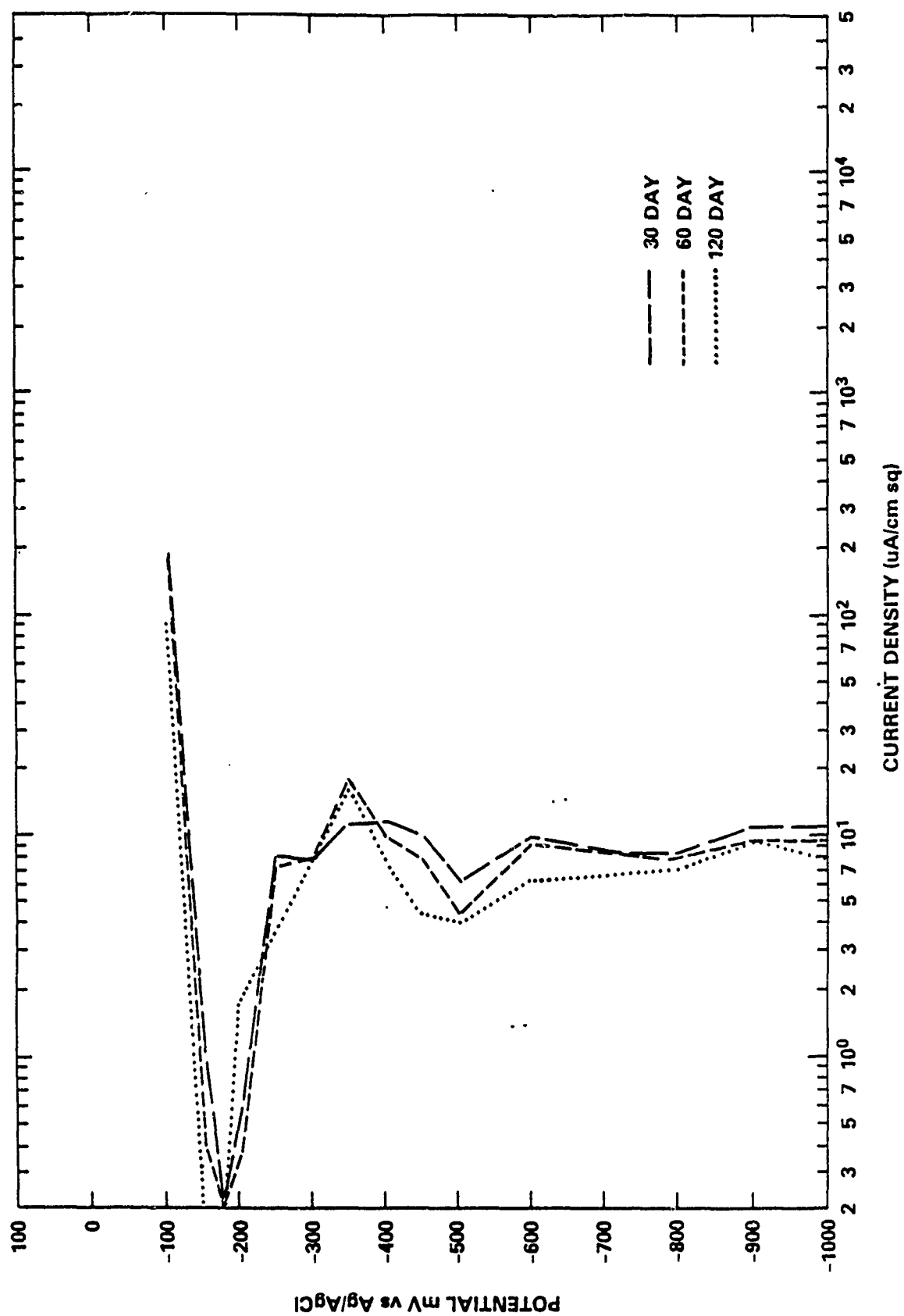Figure 2 - Potentiostatic Polarization of 90-10 Copper Nickel

34

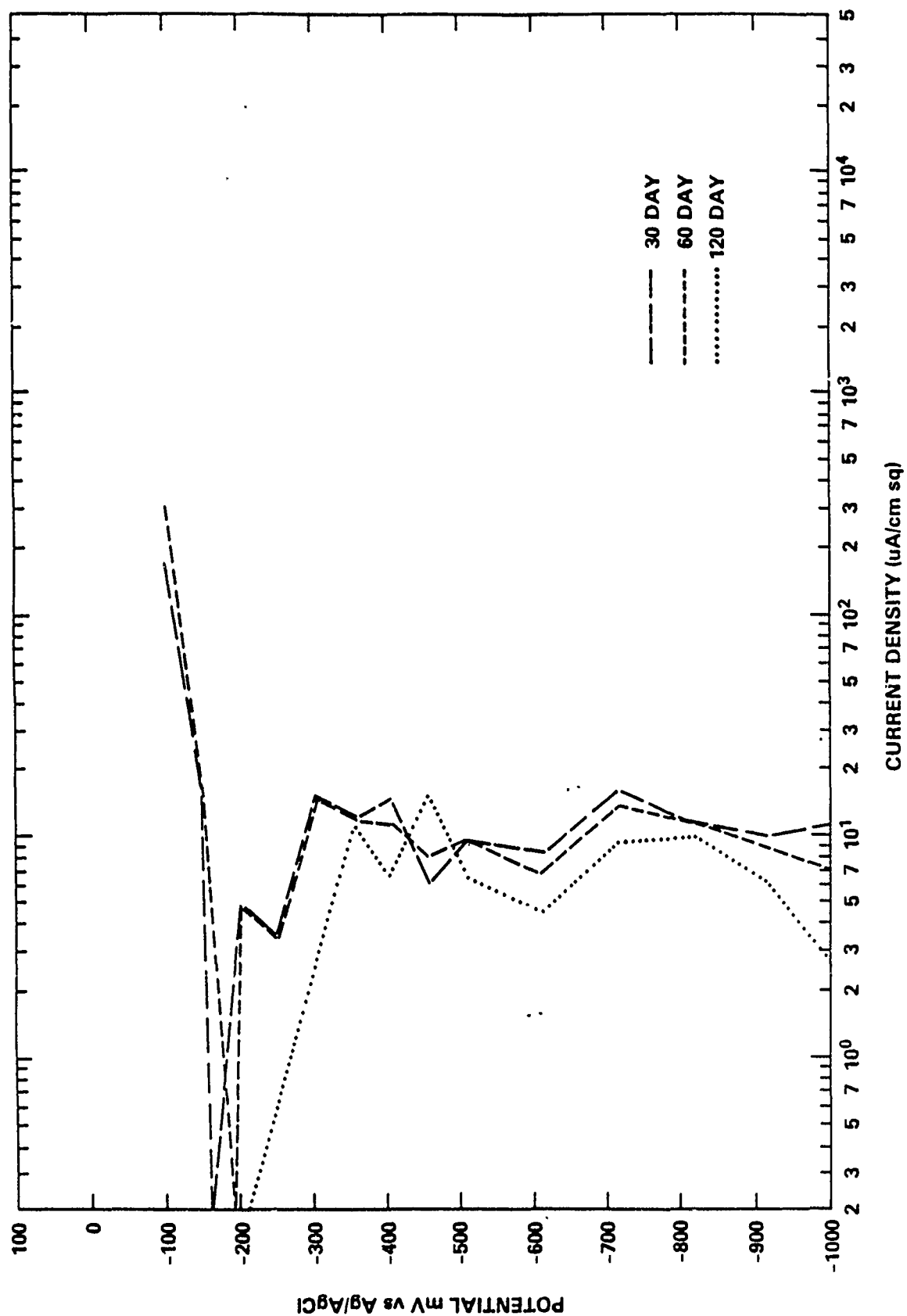Figure 3 - Potentiostatic Polarization of M-Bronze

35

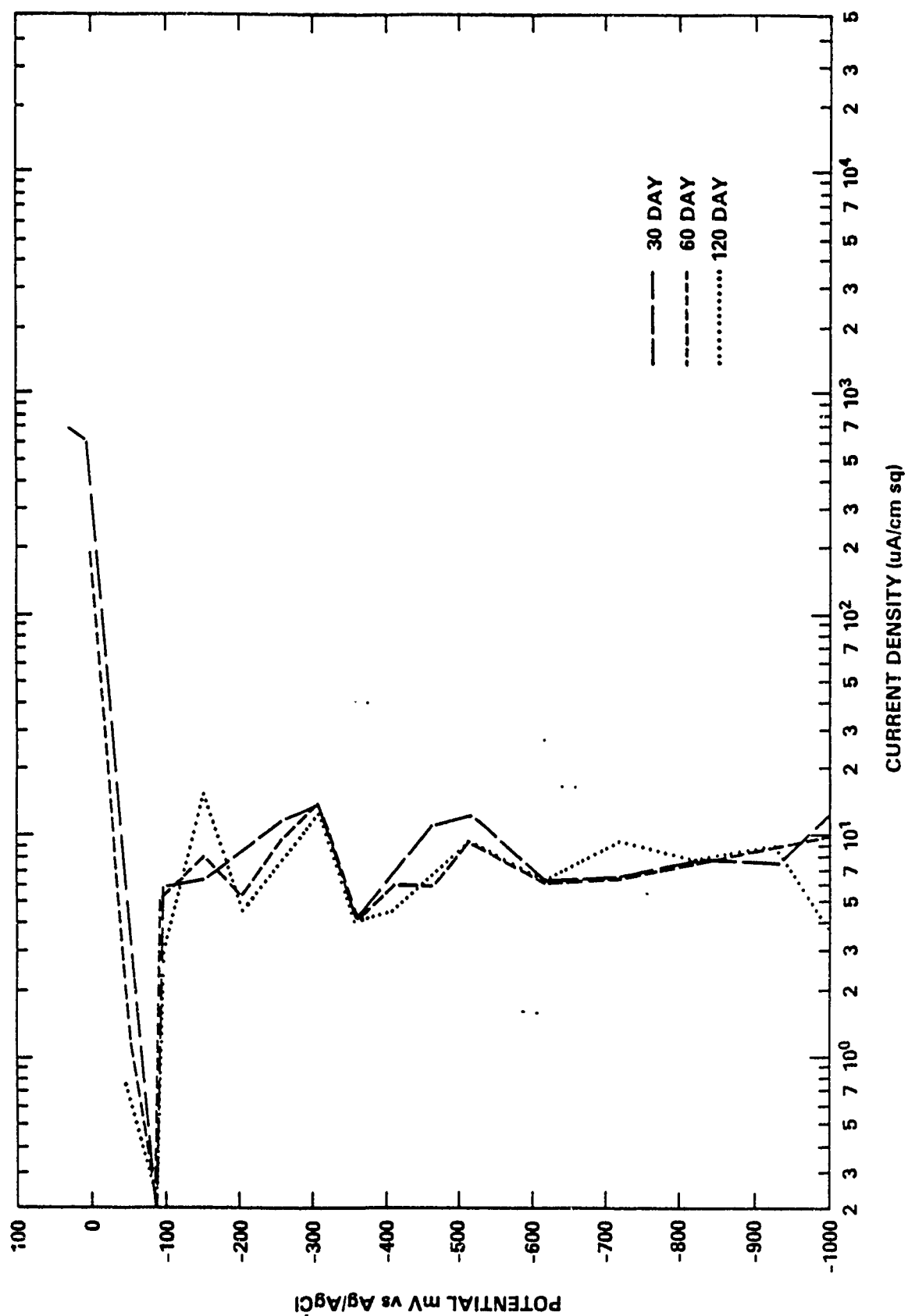Figure 4 – Potentiostatic Polarization of Nickel Aluminum Bronze

36

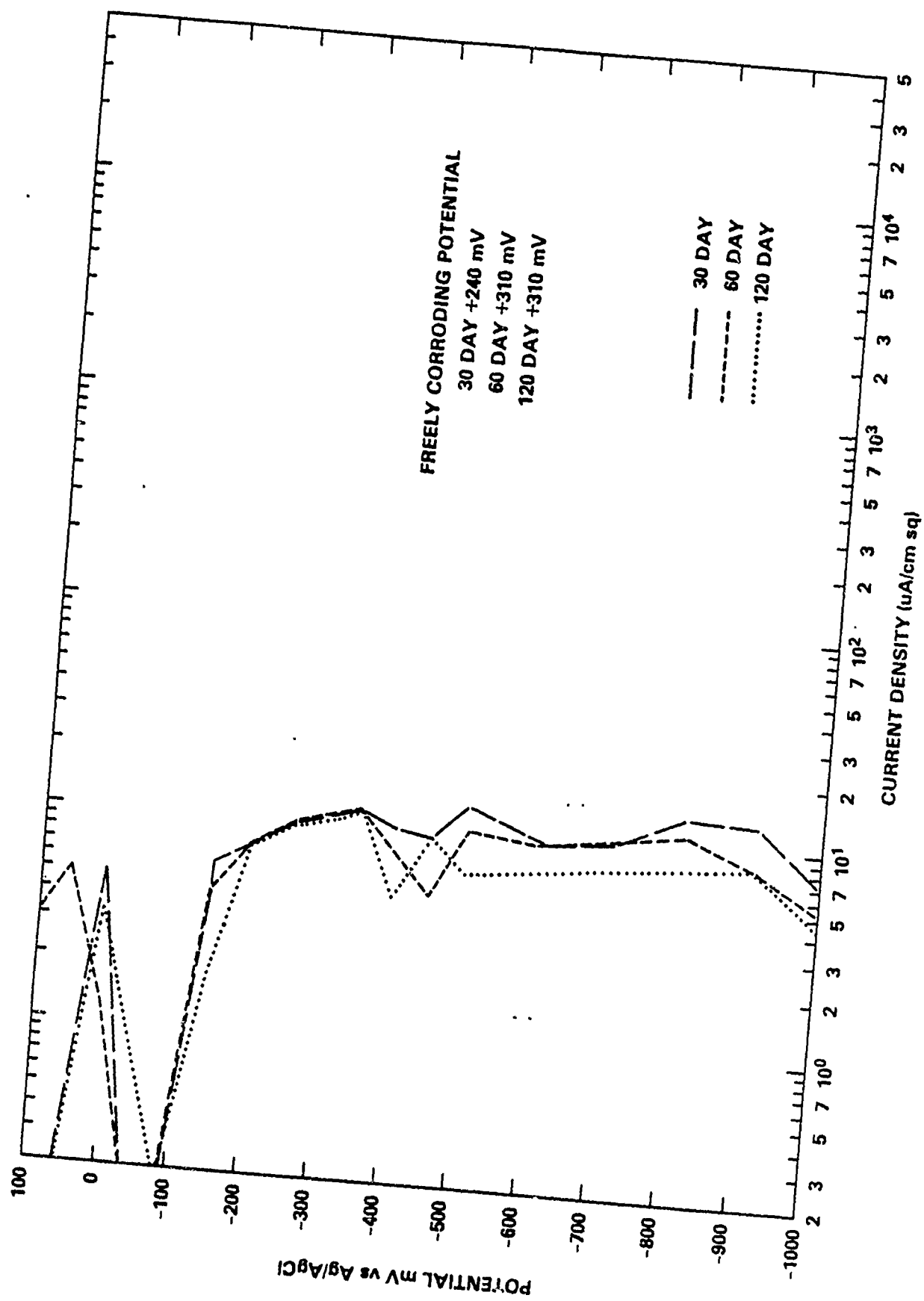Figure 5 - Potentiostatic Polarization of Monel 400
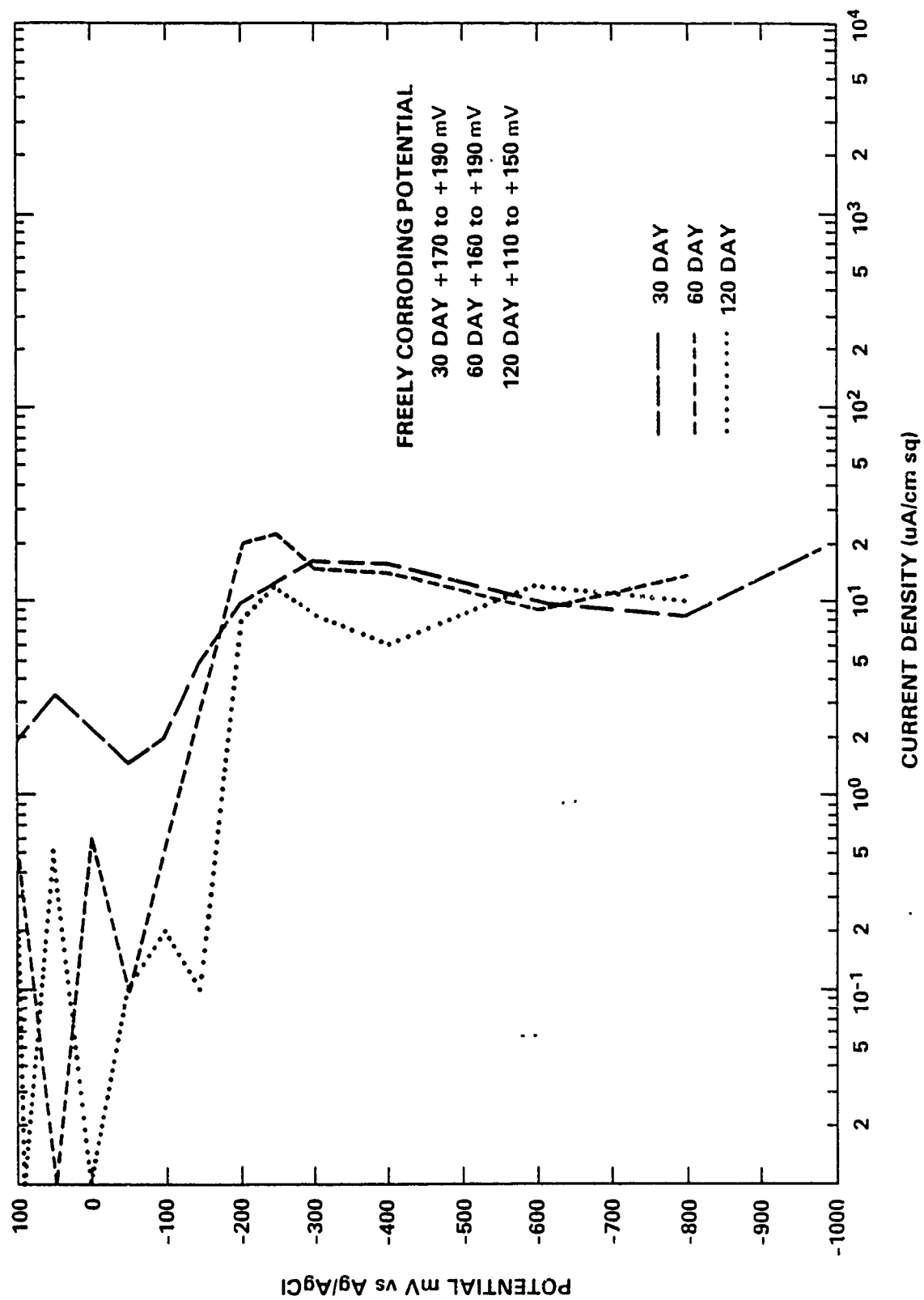
Figure 6 – Potentiostatic Polarization of INCONEL 625

FREELY CORRODING POTENTIAL

30 DAY +240 mV
60 DAY +310 mV
120 DAY +310 mV

30 DAY
60 DAY
120 DAY

CURRENT DENSITY (uA/cm sq)

POTENTIAL mV vs Ag/AgCl

38

FREELY CORRODING POTENTIAL

30 DAY +170 to +190 mV
60 DAY +160 to +190 mV
120 DAY +110 to +150 mV

30 DAY ——————
60 DAY — — — —
120 DAY ············

CURRENT DENSITY (uA/cm sq)

POTENTIAL mV vs Ag/AgCl

Figure 7 – Potentiostatic Polarization of Titanium 50
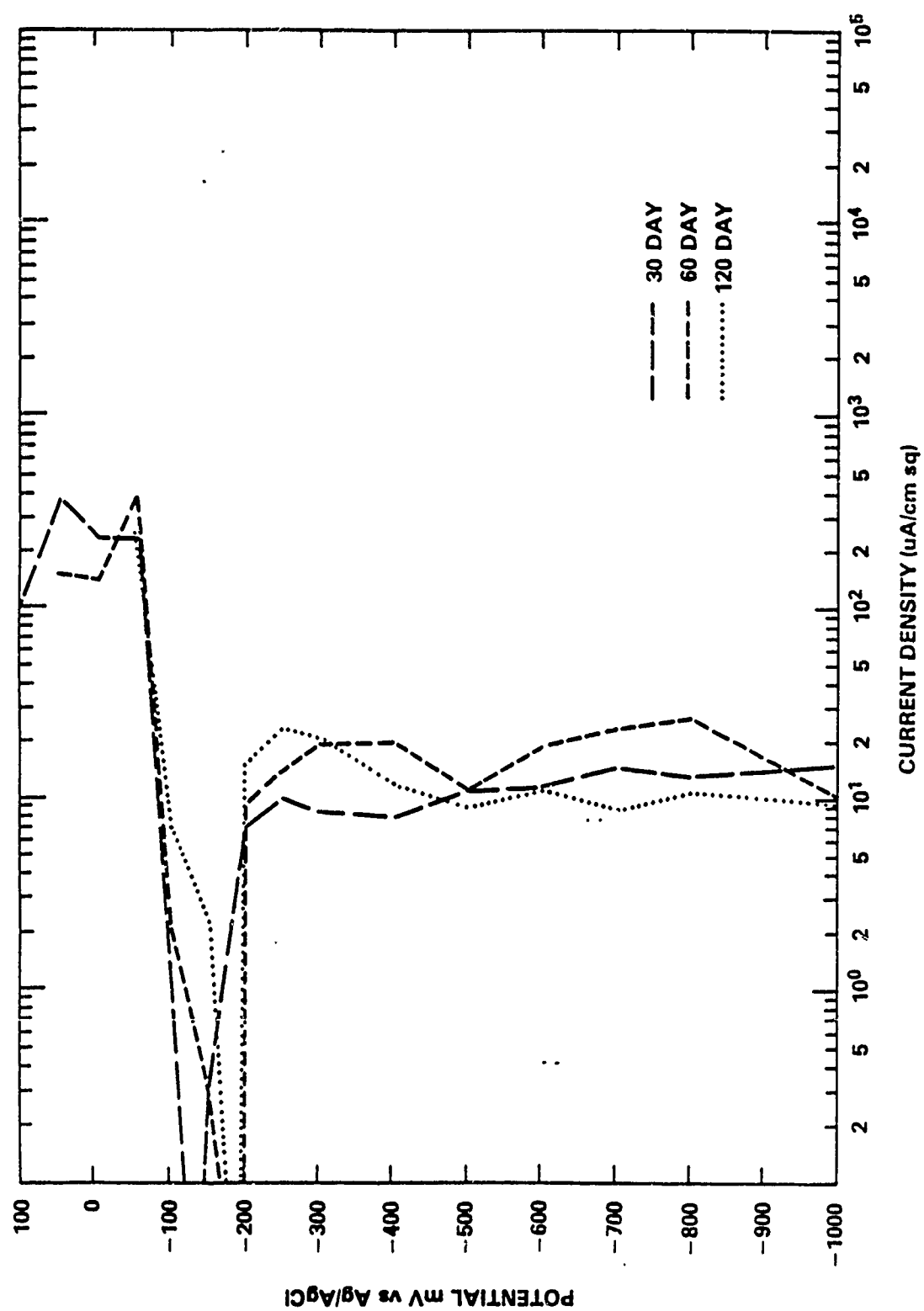
Figure 8 - Potentiostatic Polarization of 70-30 Copper Nickel
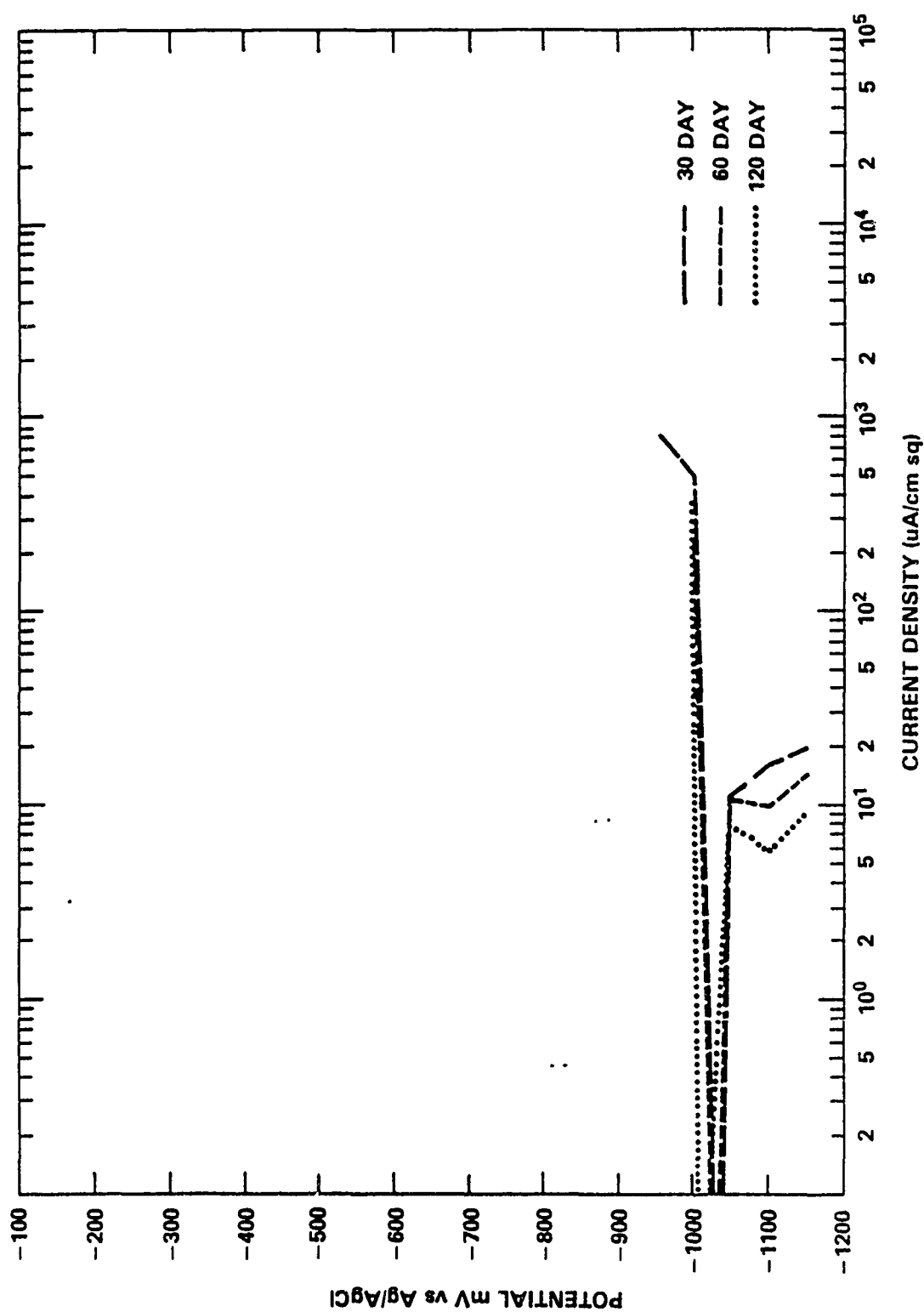
40

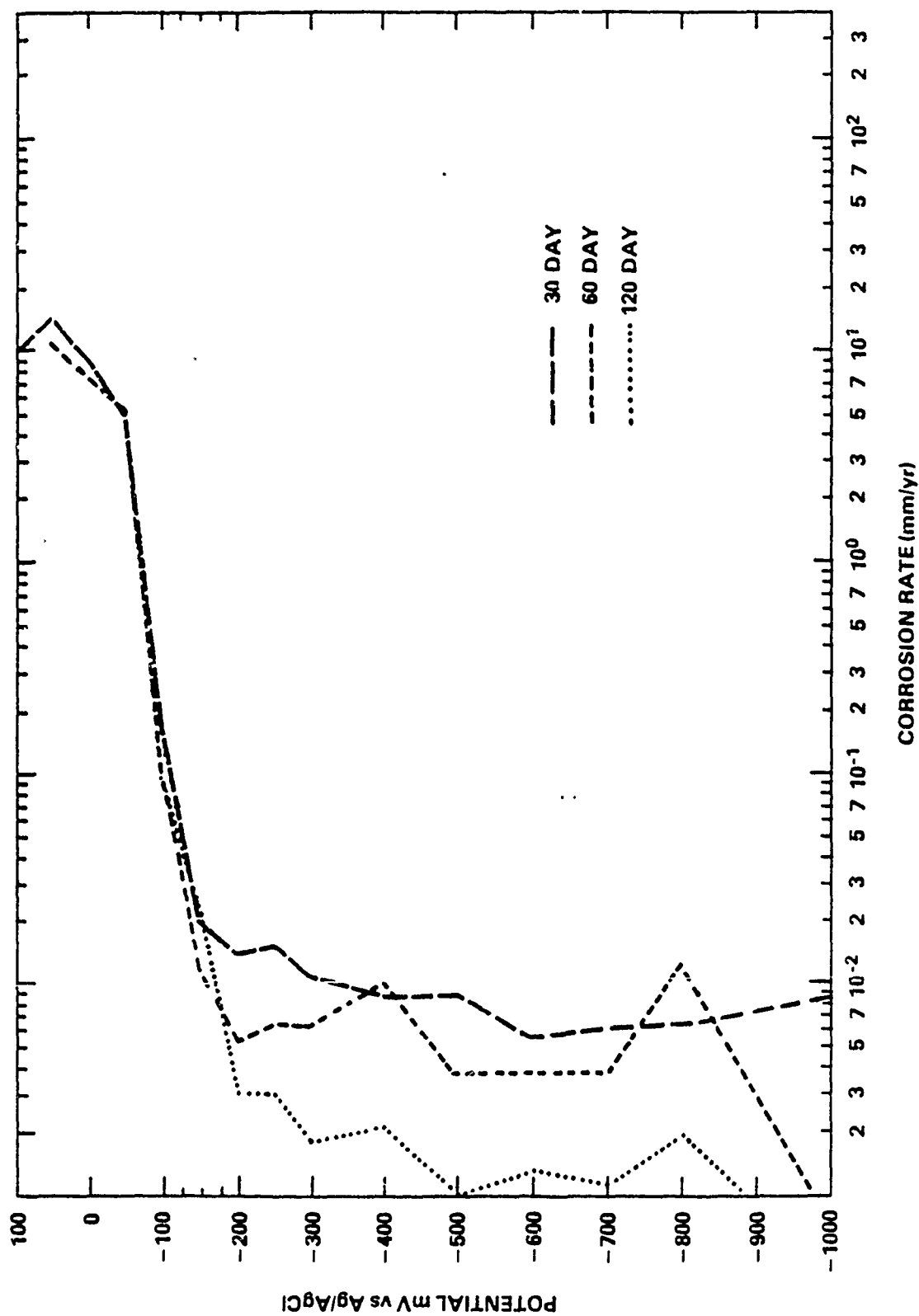Figure 9 – Potentiostatic Polarization of Anode Grade Zinc

41

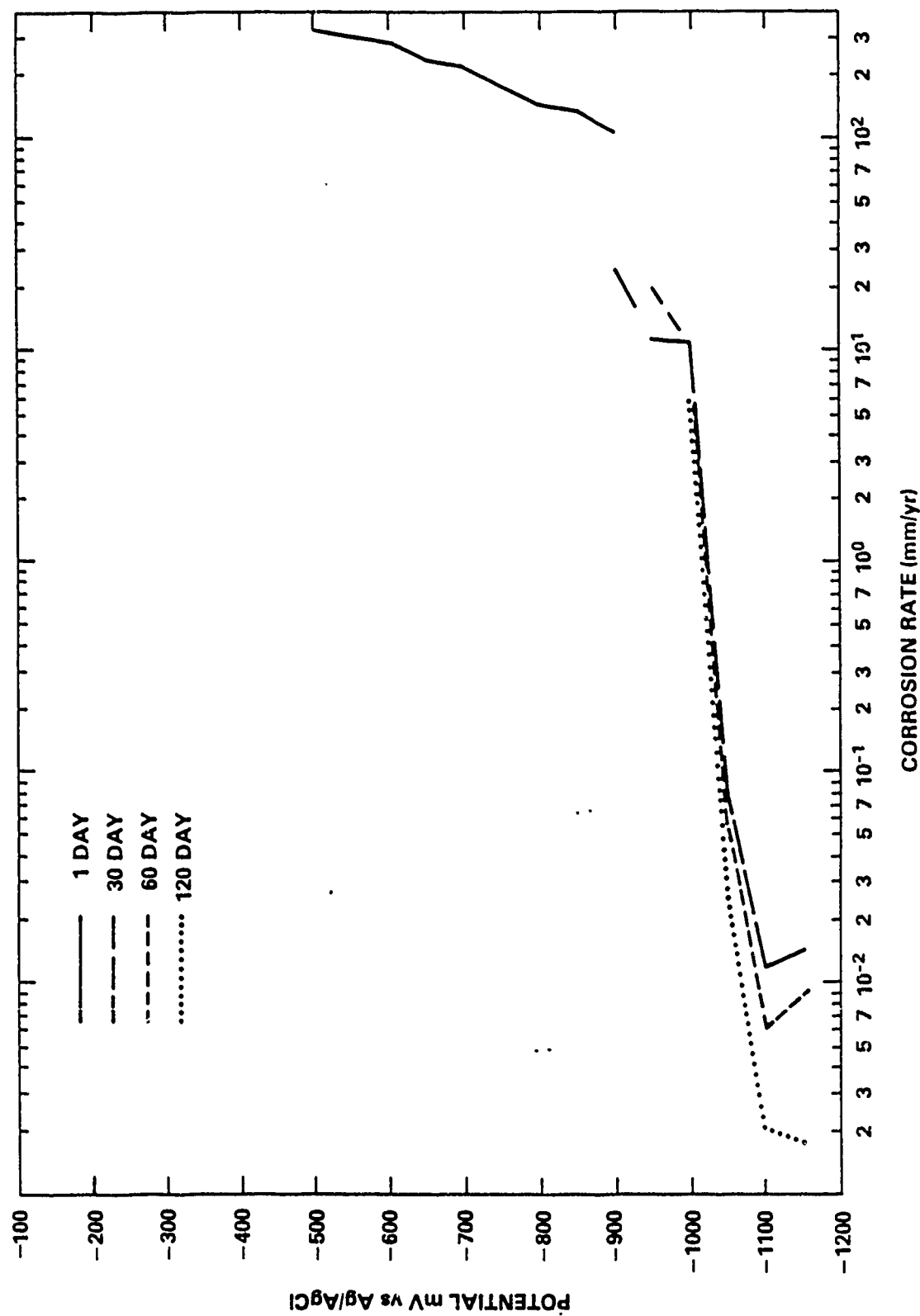Figure 10 - Corrosion of 70/30 Copper Nickel

42

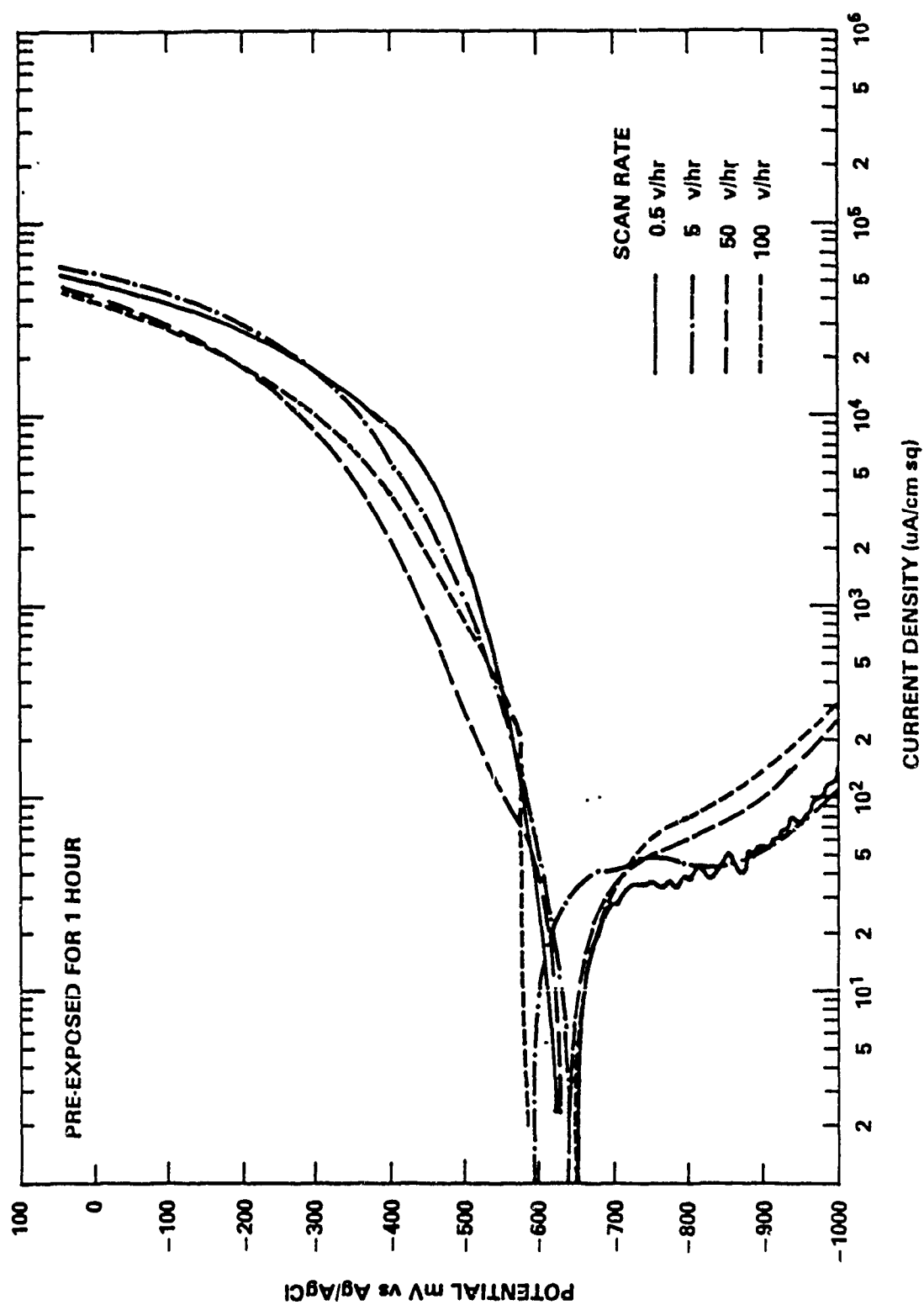Figure 11 - Corrosion of Zinc Anode Material

43

Figure 12 – Potentiodynamic Polarization of HY-80 Steel
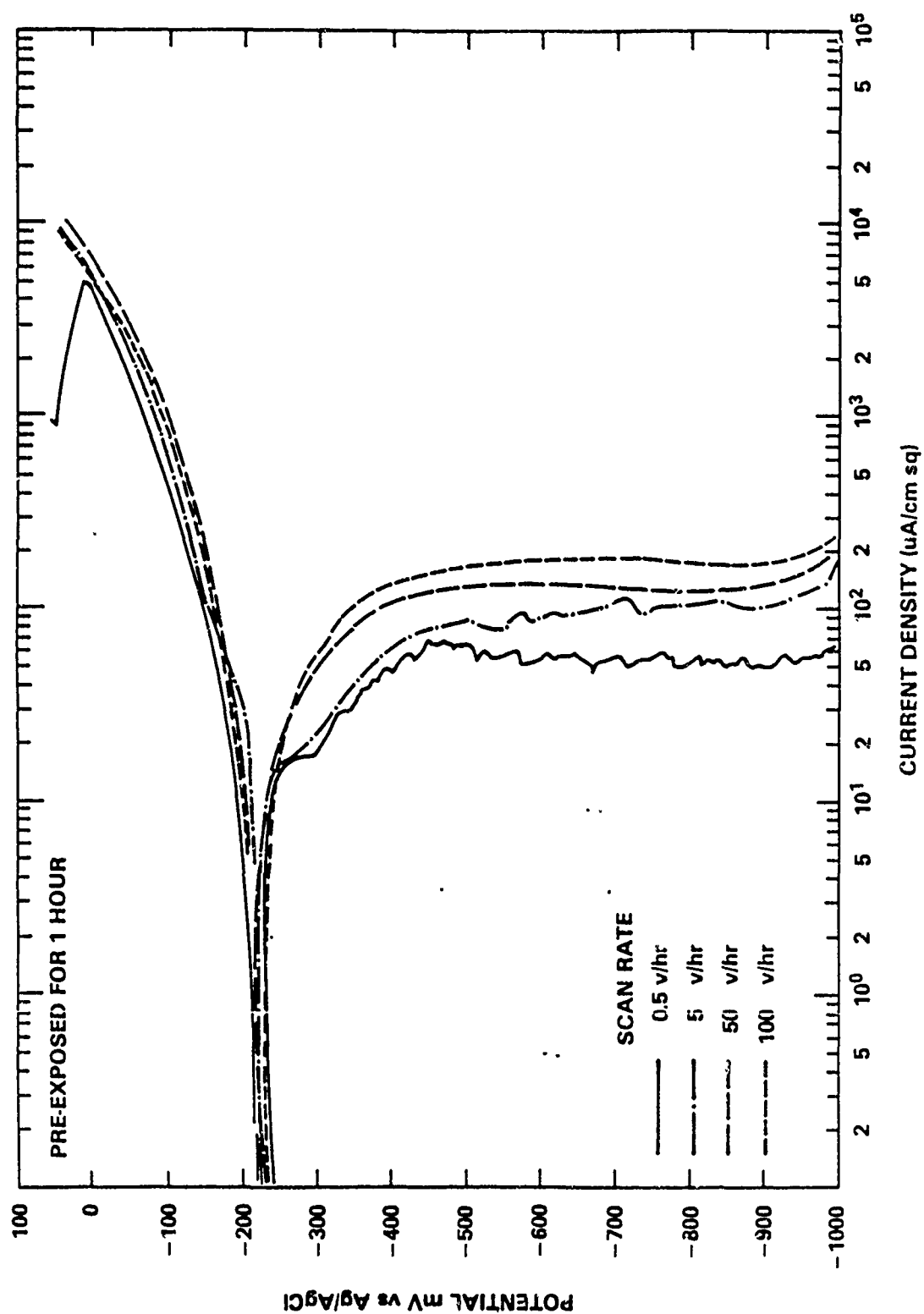After 1-Hour Pre-exposure

44

Figure 13 – Potentiodynamic Polarization of 90-10 Copper Nickel
After 1-Hour Pre-exposure

Figure 14 – Potentiodynamic Polarization of M-Bronze
After 1-Hour Pre-exposure

46

Figure 15 – Potentiodynamic Polarization of Nickel Aluminum Bronze
After 1-Hour Pre-exposure

47

Figure 16 – Potentiodynamic Polarization of Monel. 400
After 1-Hour Pre-exposure

Figure 17 - Potentiodynamic Polarization of Inconel 625
After 1-Hour Pre-exposure

49

Figure 18 – Potentiodynamic Polarization of HY-80 Steel After 120-Day Pre-exposure

Figure 19 – Potentiodynamic Polarization of 90-10 Copper Nickel
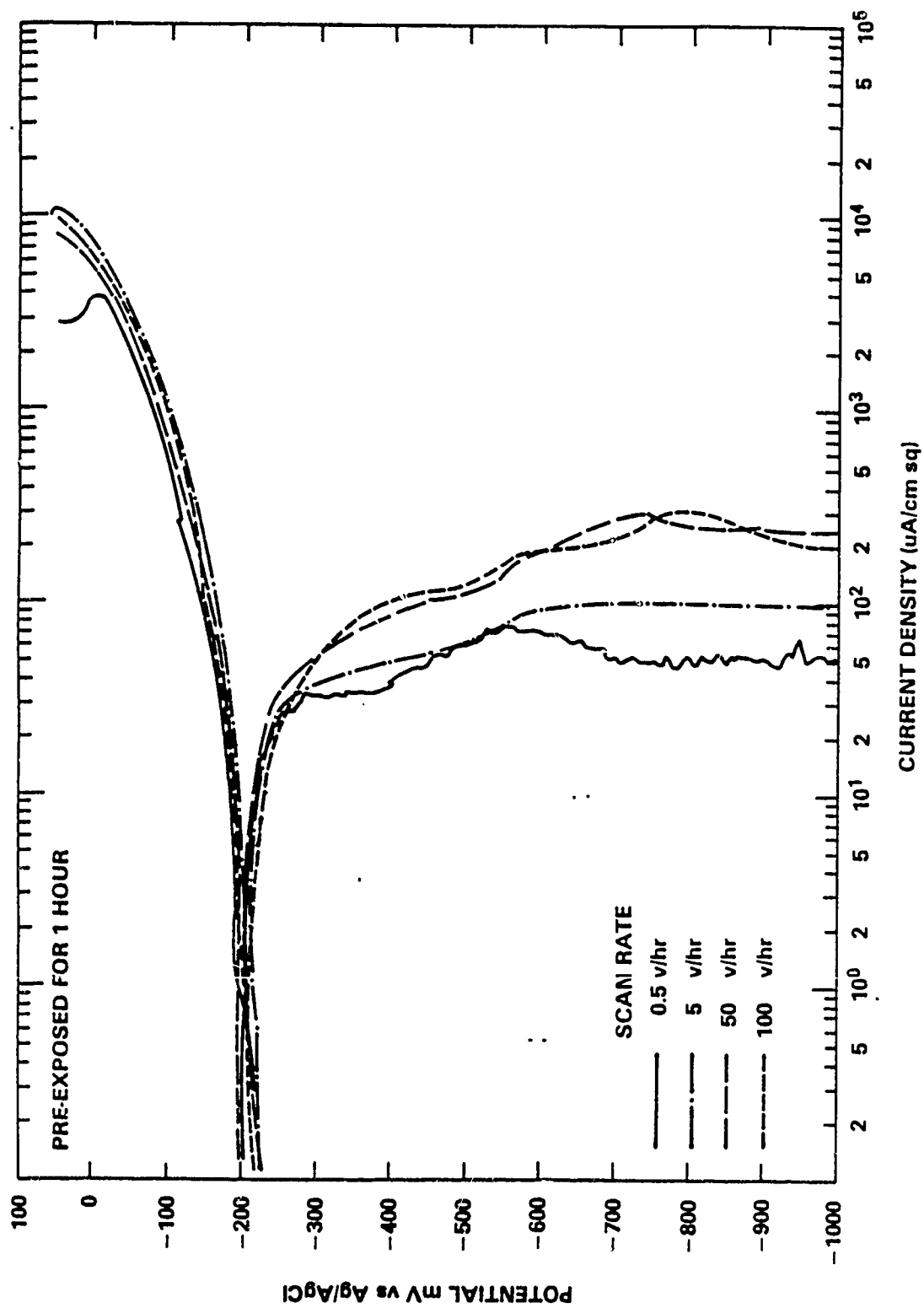After 120-Day Pre-exposure

51

Figure 20 - Potentiodynamic Polarization of M-Bronze After 120-Day Pre-exposure
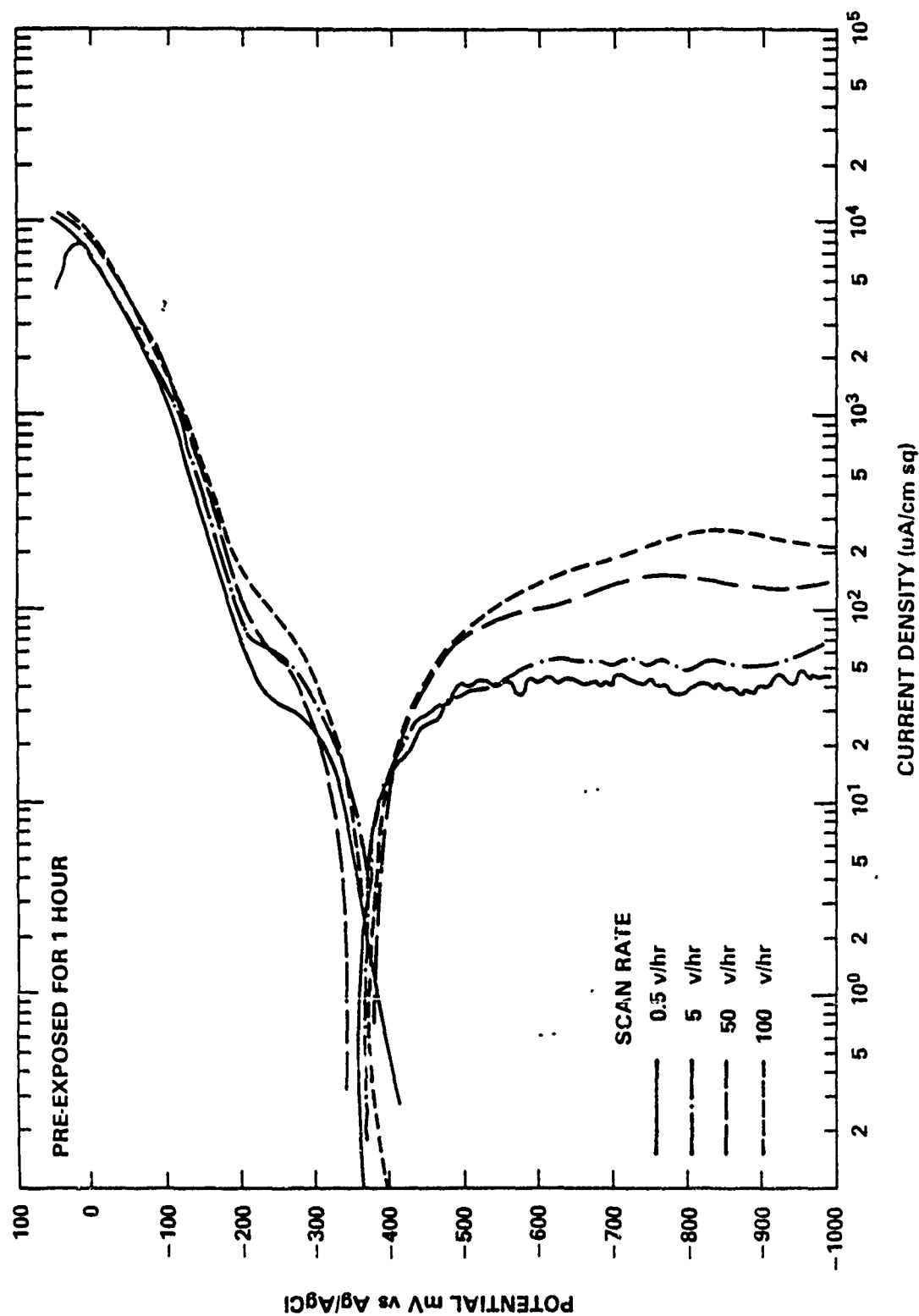
Figure 21 - Potentiodynamic Polarization of Nickel Aluminum Bronze
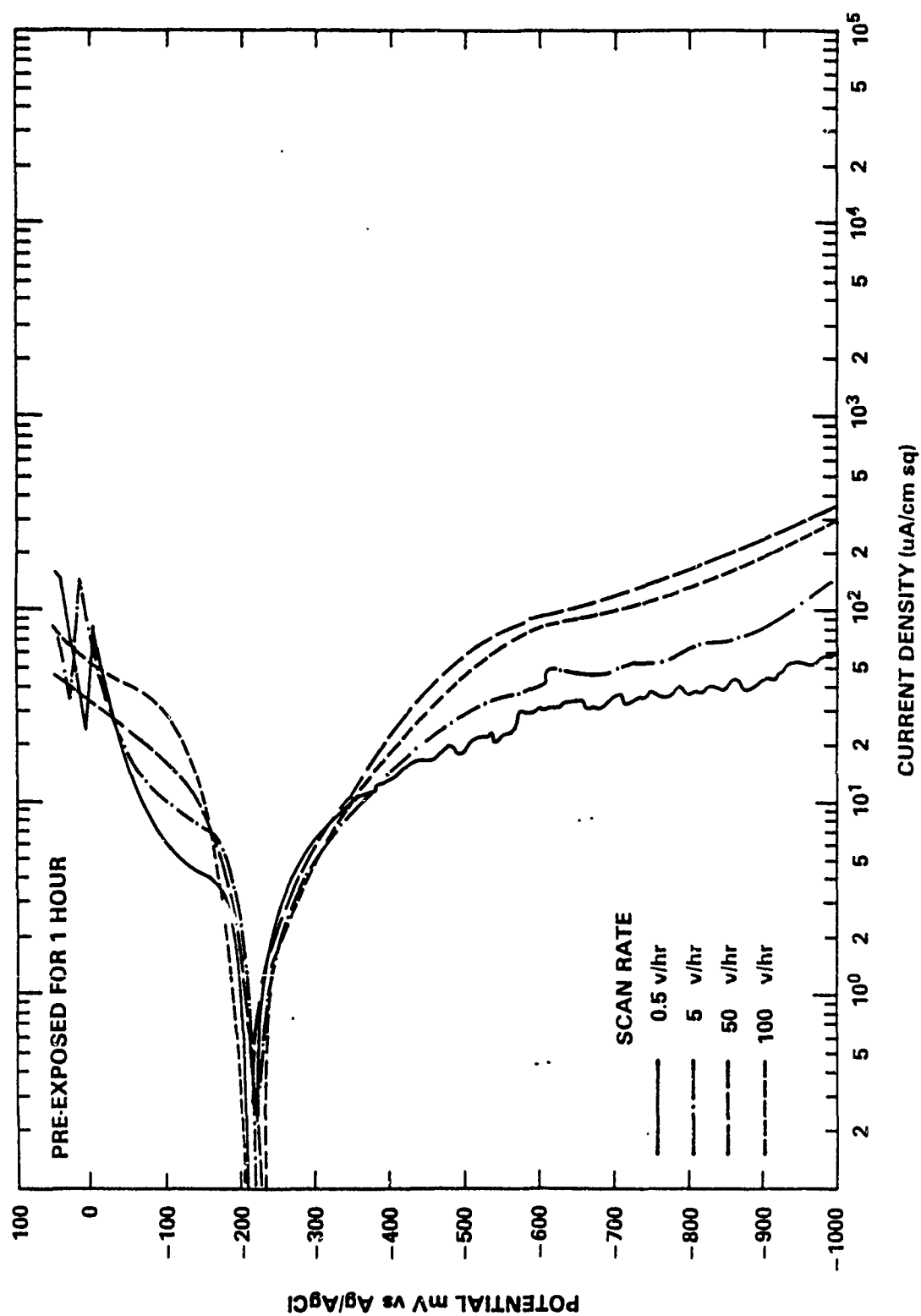After 120-Day Pre-exposure

53

Figure 22 – Potentiodynamic Polarization of Monel 400
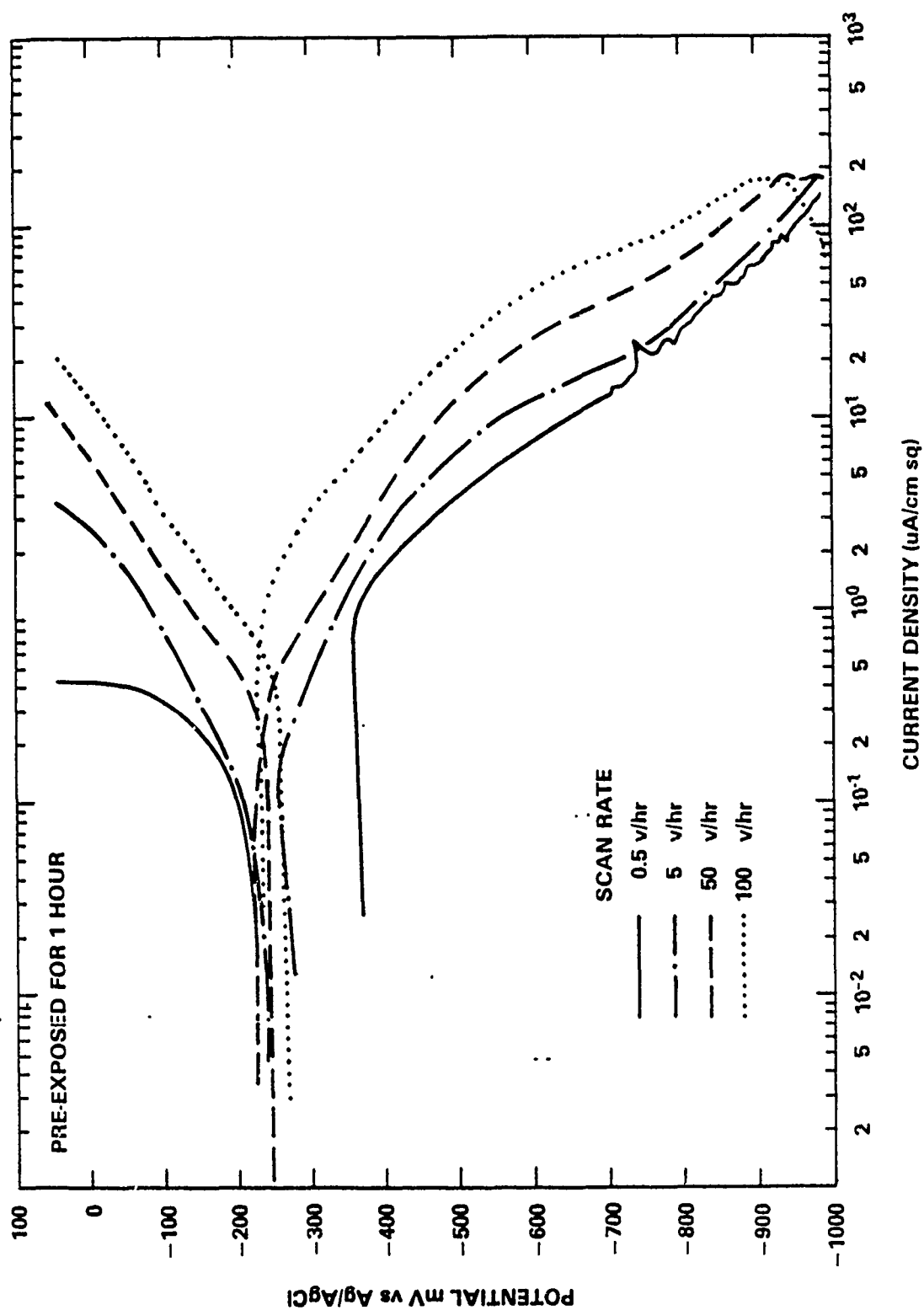After 120-Day Pre-exposure

Figure 23 – Potentiodynamic Polarization of Inconel 625
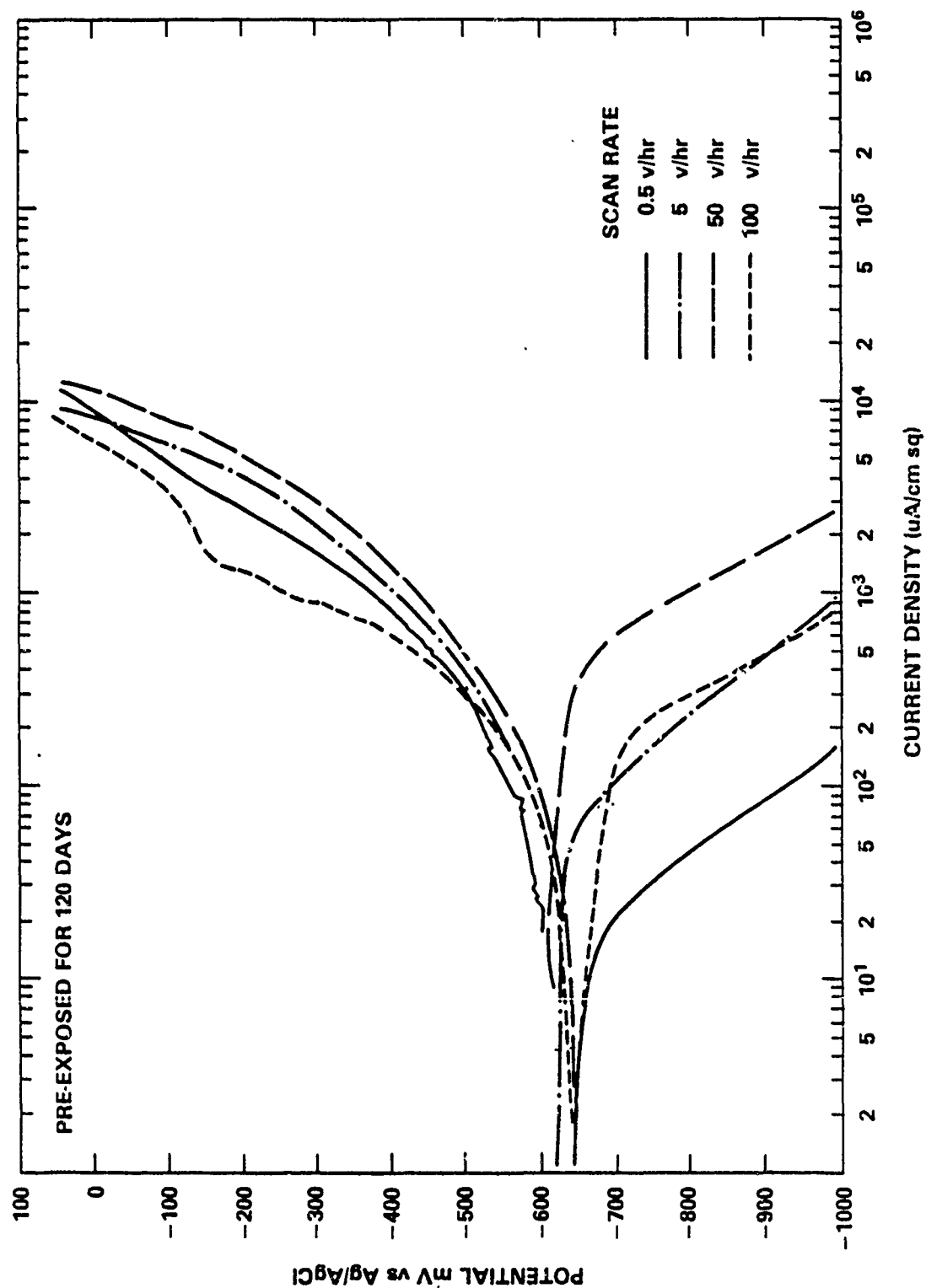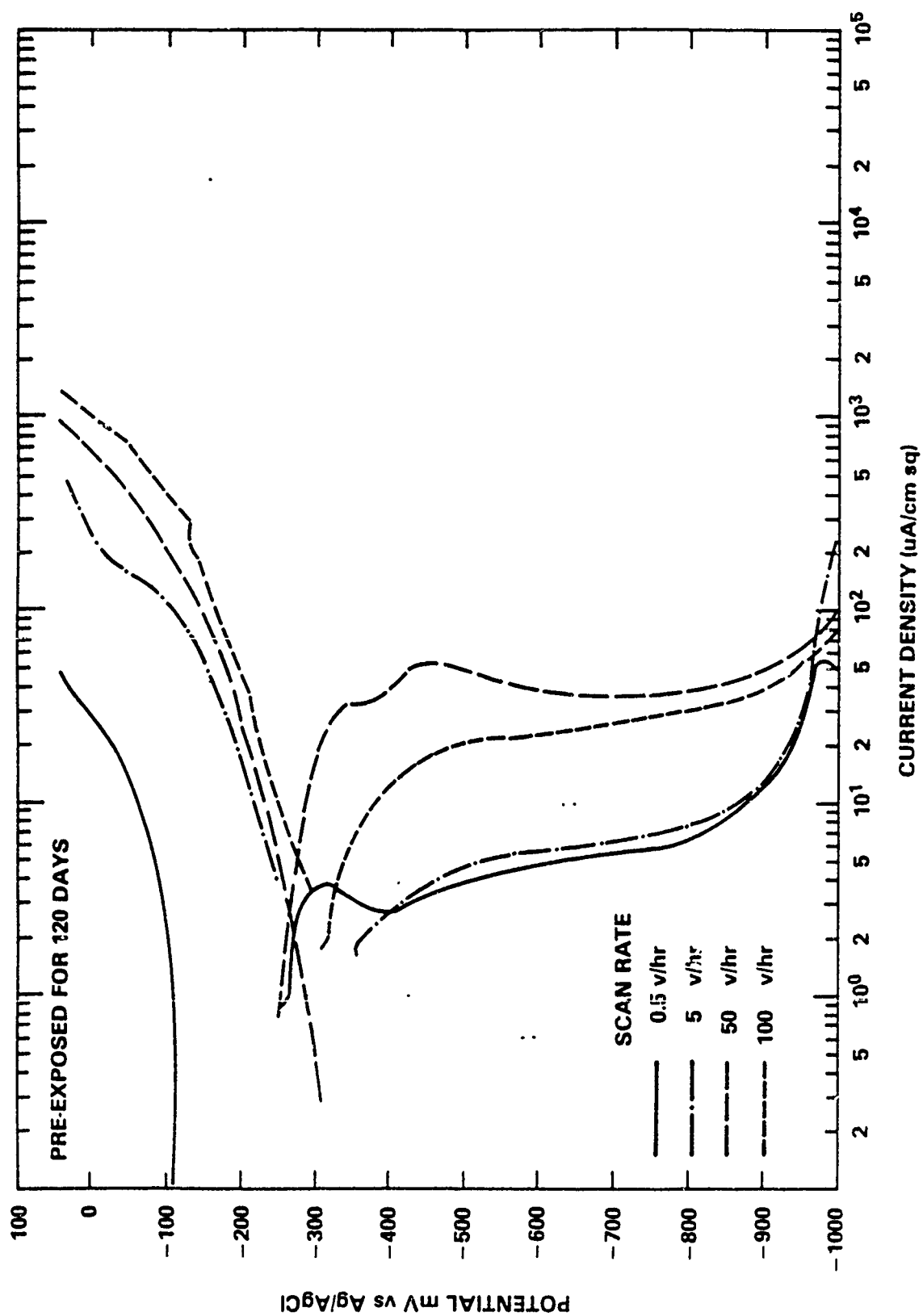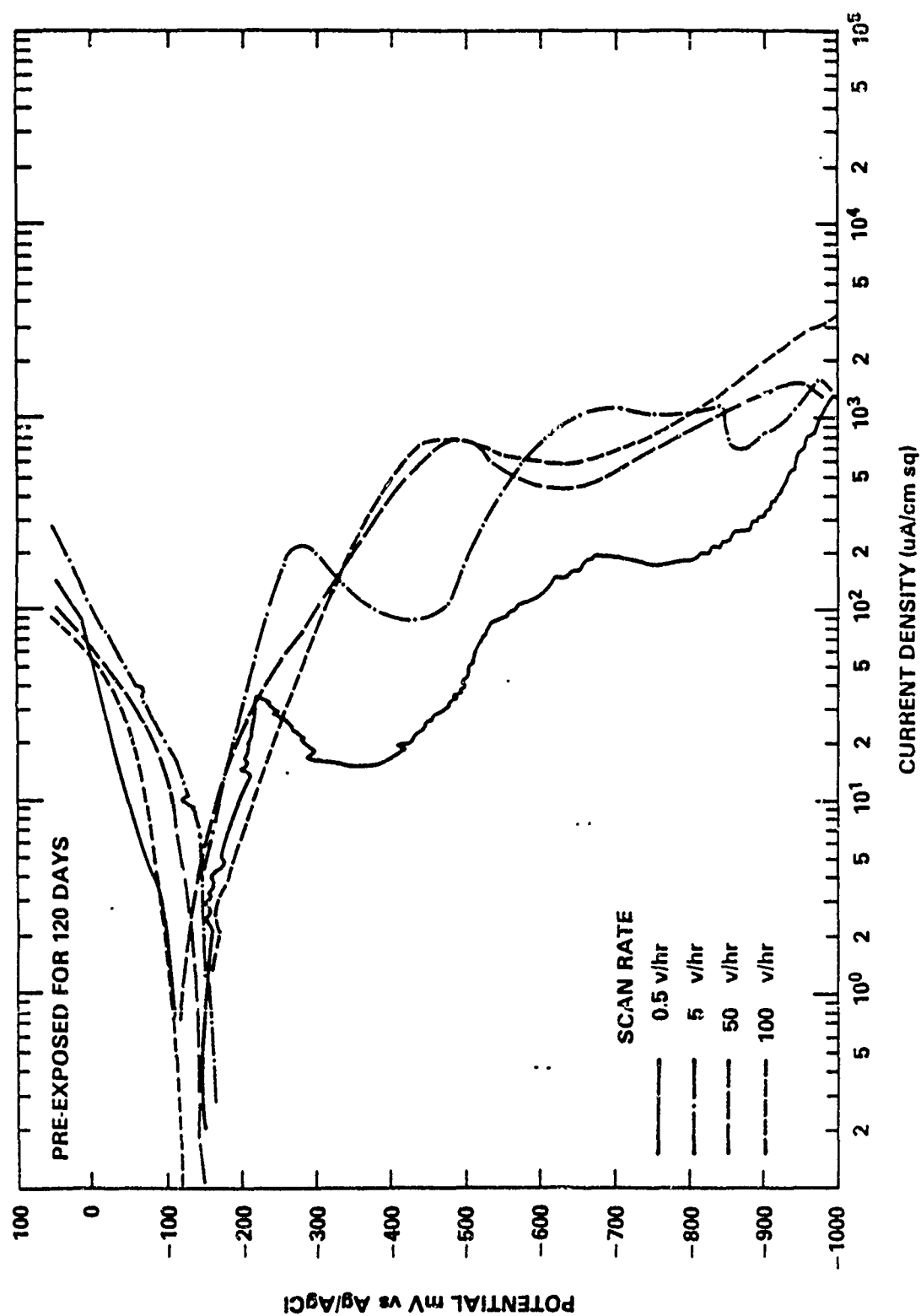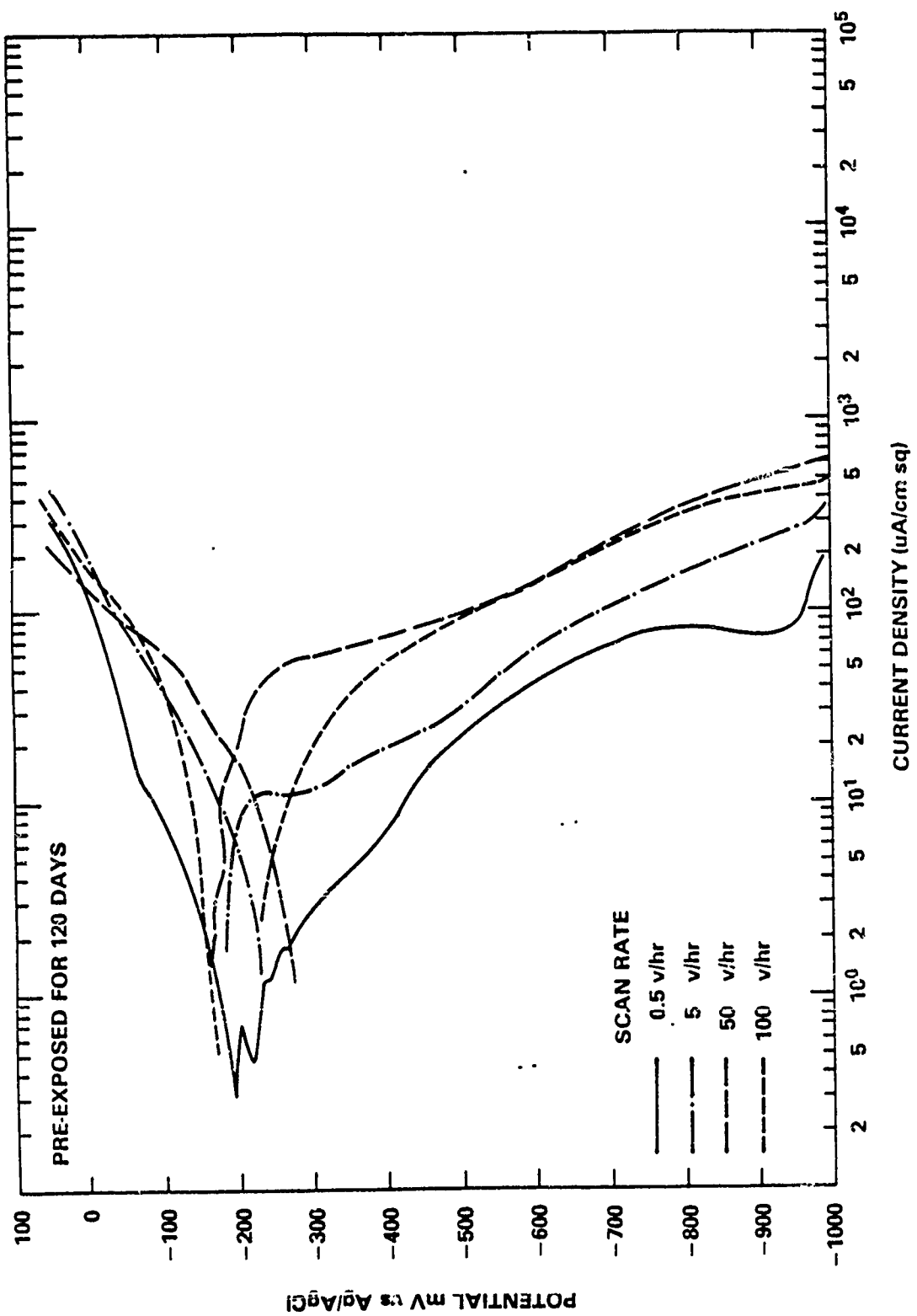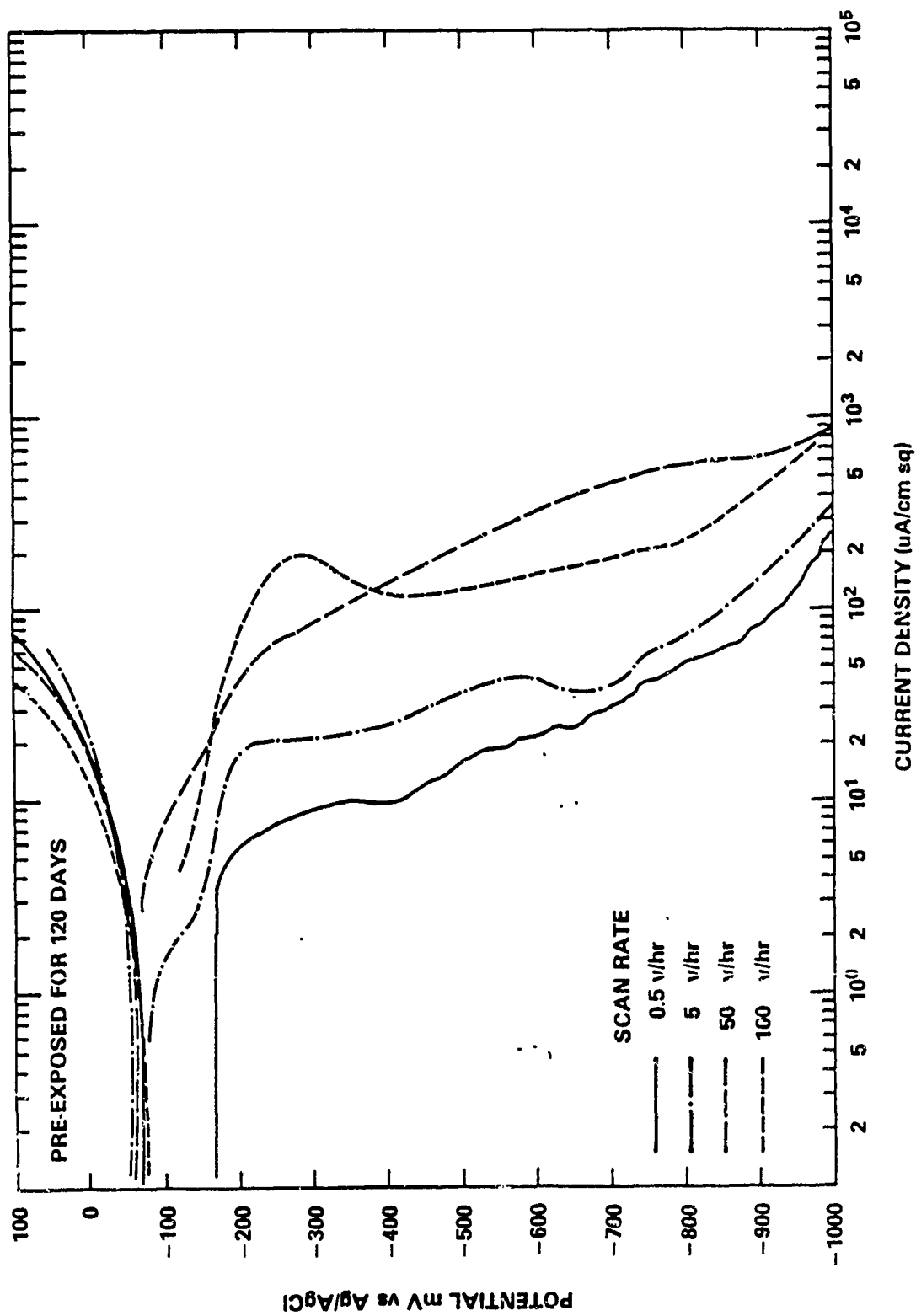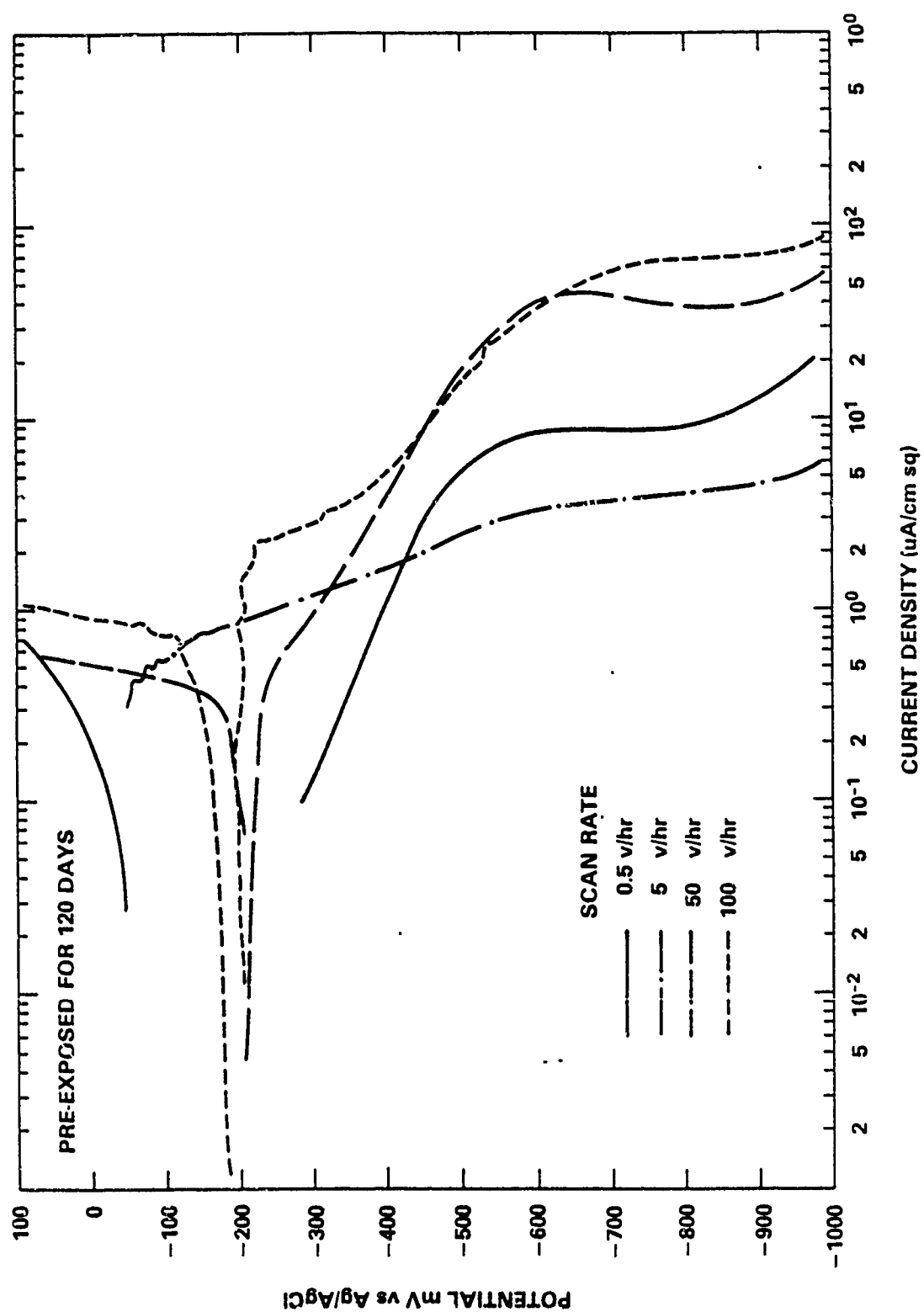After 120-Day Pre-exposure

APPENDIX

VISUAL OBSERVATIONS

CONSTANT POTENTIAL AND FREELY CORRODING SPECIMENS

Ti-50 experienced no visible attack after 30, 60, and 120 days at anodic potentials to +200 mV (Ag/AgCl). Grinding marks were still visible along with a bright metal finish on specimens exposed above -150 mV (Ag/AgCl). Below -150 mV · thin adherent tan films, presumably calcareous deposits, were observed. This film became slightly thicker with exposure duration up to 120 days. At 120 days the calcareous deposits present at -1000 mV were darker than those previously observed, with blisters present on the faces of the specimens.

Considerable general corrosion attack at anodic overpotentials was experienced by 70-30 copper nickel. At potentials of -50 to +100 mV (Ag/AgCl) a two-phase corrosion product is evident after 30 days. The thin red-brown corrosion product is presumably Cu_2O or $Cu+Cu_2O$, along with a voluminous porous green corrosion product which is loose in many places. The green deposits may consist of $CuCl_2 \cdot 3Cu(OH)_2$, $Cu(OH)_2$, or Cu_2OCL_2. After 60 and 120 days, at potentials ranging from +50 to -100 mV, a similar multiphase corrosion product formation is visible, along with general metal dissolution, leaving less than 50% of the basemetal remaining. The remaining 70-30 copper nickel is heavily etched. In addition, copper redeposition in spots is observed over the 120-day period; specimens polarized to -100 to -150 mV range display a light green tarnish and no visible signs of metal wastage. At potentials below -600 mV, the dark tan-olive tinted calcareous deposits thicken and become more adherent with exposure duration. At potentials near open-circuit (-10u to -300 mV (Ag/AgCl)), a voluminous green corrosion product is visible near the Teflon gasket, indicative of some crevice or metal ion concentration type attack.

Zinc anode specimens polarized to potentials electropositive of -950 mV (Ag/AgCl) underwent considerable general dissolution in 1-day exposures. Specimens polarized for 30 days at -950 to -1050 mV (Ag/AgCl) displayed 20% general dissolution and milky white corrosion products, probably consisting of $Zn(OH)_2$. Specimens polarized to -1150 mV displayed a tan-grey adherent film, presumably calcareous deposits. For 60-day exposures, the specimen at -950 mV displayed 90% dissolution, while specimens polarized to -1000 to -1050 mV displayed two-phase corrosion products consisting of a thick tan-grey layer, presumably $Zn(OH)_2$ and a black stain. Shallow pitting is observed under these sites. A specimen polarized at -1100 mV displays a thin adherent film, presumably calcareous deposits.

At 120 days, a specimen polarized to -1000 mV shows a porous tan corrosion product, presumably $Zn(OH)_2$, with 50% of the basemetal dissolved. At -1050 mV, a thin black stain is evident, with shallow pitting. At -1100 and -1150 mV, thin adherent grey-green films are observed; these are probably calcareous deposits.

BIMETAL AND MULTIMETAL COUPLES

In general, for bimetallic couples where the anode material is zinc, cathode materials display calcareous deposition and no general surface wastage. HY-80 displayed thick and spongy calcareous layers over the 120-day period, while nickel-aluminum-bronze, 90-10 Cu-Ni, Monel, Ti-50, and Inconel 625 displayed thin adherent calcareous layers. Ti-50, Inconel 625, and Monel showed no visible signs of attack, while nickel-aluminum-bronze and 90-10 Cu-Ni displayed a uniform surface tarnish, in addition to the thin calcareous layer. HY-80 showed slight surface attack at blisters which formed in the thick calcareous layers after 60 days. For multimetal couples containing zinc as the most prominent anode material, essentially the same observations are made for the various cathode materials. In all cases, zinc anode material displayed a spongy white corrosion product, probably $Zn(OH)_2$. Beneath the voluminous white corrosion product, a dark stain is observed. Surface wastage, mainly in the form of shallow (1 to 2-mm depth) by 3-mm-diameter pits, are observed on zinc specimens. For Monel couple to Ti-50, pitting and crevice attack with voluminous green product and bright metal; boldly-exposed surfaces are observed on Monel. For 70-30 Cu-Ni coupled to Ti-50, a multiphase corrosion product consisting of a voluminous green product at crevices, a red-brown tarnish and a green corrosion product is observed on 70-30 Cu-Ni. A similar appearance is displayed for 70-30 Cu-Ni coupled to Inconel 625 and to Monel. Nickel-aluminum-bronze coupled to Inconel 625 displays a multiphase corrosion product consisting of a voluminous green product at the washer, a red-brown tarnish, and other corrosion products on boldly exposed surfaces. In all cases Inconel 625 and Ti-50 displayed no attack or tarnish, but slight calcareous formation is observed. For M-bronze coupled to 70-30 Cu-Ni and M-bronze coupled to 90-30 Cu-Ni, both alloys displayed tarnishes and voluminous corrosion products at washers. Tables A.1 and A.2 summarize observations for individual cases.

TABLE A.1 — BIMETALLIC COUPLE VISUAL OBSERVATIONS

Galvanic Couple	Product Formation	Form of Corrosion Visible	Product Formation	Form of Corrosion Visible	Product Formation	Form of Corrosion Visible
HY80	Slight calcareous	None	Blistering calcareous	None	Blistering calcareous	None
Zinc	Spotty milky ZnOH₂	General	Milky and black stains	Pitting	Milky ZnOH₂ and black stain	Pitting
NAB	Slight calcareous	None	Calcareous	None	Calcareous	None
Zinc	Spotty milky ZnOH₂	General	Milky ZnOH₂ and black stain	Pitting	Milky ZnOH₂ and black stain	Pitting
90-10 CuNi	Slight calcareous	None	Calcareous	None	Tarnish & calcareous	None
Zinc	Spotty milky ZnOH₂	General	Milky ZnOH₂ and black stain	Pitting	Milky ZnOH₂ and black stain	Pitting
T1-50	None	None	None	None	Slight calcareous	None
Monel	Green corr. pro. at gasket	Pitting at gasket	Voluminous green at edges, crevices	Pitting	Voluminous green at edges, crevices	Crevice attack
T1-50	None	None	None	None	Slight calcareous	None
70-30 CuNi	Voluminous green, at crevice and red	Slight crevice shallow pitting	Voluminous green, red redeposition of copper	Shallow pitting	Brown tarnish voluminous green	General
Monel	None	None	None	None	Calcareous	None
70-30 CuNi	Voluminous Green at crevice	Slight crevice	Green at crevice red tarnish	Slight crevice	green-brown tarnish voluminous green	Crevice attack
IN 625	None	None	None	None	Calcareous	None
70-30 CuNi	Voluminous green at crevice red on surface	Crevice attack shallow pitting	Green at crevice red tarnish	Slight crevice	Green-brown tarnish voluminous green	Crevice attack
IN 625	Slight calcareous	None	Calcareous	None	Calcareous	None
NAB	Green around washer spotted red-brown	Slight general	Green at crevices spotted red	Slight general attack	Voluminous green tarnish red-brown	Crevice attack
M-Bronze	Voluminous green red brown	Slight crevice attack	Green at crevice red tarnish	Slight crevice attack	Red-brown tarnish Voluminous green	Slight crevice attack
70-30 CuNi	Tarnish	None	Tarnish	None	Voluminous green red-green tarnish	Slight crevice attack
M-Bronze	Voluminous green at crevice red brown	Slight crevice attack	Red-brown green at crevice tarnish	Slight crevice attack	Red-brown tarnish	Slight crevice attack
90-10 CuNi	Tarnish	None	Green at crevice yellow tarnish	None	Voluminous green Red-green tarnish	Slight crevice attack

59

TABLE A.2 - MULTIMETAL COUPLE VISUAL OBSERVATIONS

Galvanic Couple	30 Day Product Formation	Form of Visible Corrosion	60 Day Product Formation	Form of Visible Corrosion	120 Day Product Formation	Form of Visible Corrosion
HY-80	White calcareous	None	White calcareous with blisters	None	White blisters with black underneath calcareous deposits	None
NAB	Silting	None	Thin calcareous	None	Thin calcareous	None
Zinc	White $ZnOH_2$	General corrosion	Milky white corrosion product with $Zn(OH)_2$	Pitting and general attack	White-tan deposits and black tarnish	Shallow pitting/general attack
TI-50	None	None	Bright metal, slight calcareous deposition	None	Bright metal, slight calcareous	None
IN 625	None	None	Bright metal, slight calcareous deposition	None	Bright metal, slight calcareous	None
70/30	Voluminous green red-brown stain	General corrosion	Voluminous green, brown-red oxide	Incipient	Rust brown, uniform deposit green at code and top edge	Shallow crevice/general attack
TI-50	35% Calcareous	None	Bright metal/calcareous	None	Adherent thin calcareous	None
70/30	25% Calcareous	None	Bright metal/calcareous	None	Adherent slight tarnish	None
Zinc	Spotted white $ZnOH_2$	General corrosion	White deposits at spots	Pitting/general	Tan corrosion pro $ZnOH$, grey tarnish	Pitting/general attack
Monel	Calcareous	None	Uniform calcareous with blisters	None	Blistering, calcareous deposits	None
90-10	Calcareous	None	Adherent calcareous	None	Calcareous deposits tarnish	None
Zinc	Spotted white corrosion	General corrosion	White corrosion product	Pitting/general	Tan deposits, dark tarnish	Pitting/general attack
IN 625	Calcareous	None	Voluminous white tan deposits	None	Calcareous deposits with blisters, dark blotches	None
NAB	Slight calcareous	None	60% Thin calcareous	None	Uniform tan calcareous	None
Zinc	Spotted white corrosion product	General corrosion	White deposits, black tarnish uniformly distributed	Pitting/general	Tan deposits $ZnOH_2$ with grey tarnish	Pitting/general attack
IN 625	None	None	Bright metal/calcareous	None	Light calcareous deposits	None
Monel	None	None	Bright metal/thin calcareous	None	Green deposits at washer, bright metal	Crevice
70/30	Voluminous green Corrosion product	Incipient	Voluminous green deposits at crevice/brown-red deposits on face	Crevice/general	Voluminous green/red-brown thin deposits bright metal below	Crevice/general
Monel	None	None	Bright metal/slight calcareous	None	Bright metal/slight calcareous tarnish	None
TI-50	None	None	Bright metal/slight calcareous	None	Slight calcareous	None
NAB	Green product around crevice, red-brown product	Incipient	Green tarnish, voluminous corrosion at washer/red brown	Crevice/general	Uniform surface stain-tarnish voluminous brown, corrosion product, voluminous green at crevice	Crevice/general
IN 625	Calcareous	None	Bright metal/slight calcareous	None	Uniform thin calcareous	None
NAB	Green product at crevices/spotted red-brown around	None	Green tarnish, green voluminous at crevices, red-brown on face sheets	Crevice/general	Voluminous rust-brown product in spots Voluminous green at crevice	Crevice/general
70/30	Green product around washer	None	Slight calcareous, some tarnish, green voluminous at crevice	Crevice	tarnish, voluminous green at crevice	Crevice/general

60

REFERENCES

1. Treseder, R.S. Ed, <u>NACE Corrosion Engineer's Reference Book</u>, NACE, p. 62-66 (1980).

2. LaQue, F.L., <u>Marine Corrosion Causes and Prevention</u>, J. Wiley & Sons, Inc. p. 179 (1975).

3. Aylor,D.M. and H.P. Hack, "Comparative Galvanic Corrosion Effects of Noble Metals on Bronze in Seawater" Corrosion 82, Houston, TX (Mar 22-26 1982).

4. H.P. Hack and W.L. Adamson, "Analysis of Galvanic Corrosion Between a Titanium Condenser and Copper-Nickel Piping System, DTNSRDC Report 4553 (Jan 1976).

5. Fontana, M.G., and M.D. Greene, <u>Corrosion Engineering</u>, McGraw-Hill Inc., New York, N.Y., pp. 330-335 (1978).

6. Uhlg, H.H., <u>Corrosion and Corrosion Control</u>, John Wiley & Sons, Inc., New York, N.Y., pp. 106-108 (1971).

7. Baboian, R., "Predicting Galvanic Corrosion Using Electrochemical Techniques," <u>Electrochemical Techniques for Corrosion</u>, National Association of Corrosion Engineering, Houston, TX, pp. 73-78 (1977)

8. Hack, H.P. "Galvanic Corrosion Prediction Using Long-Term Potentiostatic Polarization Curves," Paper No. 73, Corrosion 83, Anaheim, CA (18-22 Apr 1983).

9. Scully, J.R. and P.J. Moran, "Extended Abstracts of the Electrochemical Society," October meeting, Washington, D.C. (1983)

10. Mansfeld, F., "The Effect of Uncompensated Resistance on the True Scan Rate in Potentiodynamic Experiments," <u>Corrosion</u>, Vol. 38, No. 10 (1982).

11. ASTM Standard G1-81, Vol. 10, p. 871 (1982).

12. ASTM Standard G5-72, Vol. 10, p. 666 (1977).

13. Ambrose, J.R., A.E. Yaniv, and U.R. Lee, "Nucleation, Growth, and Morphology of Calcareous Deposits on Steel in Seawater," Paper No. 60, Corrosion 83, Anaheim, CA (Apr 18-22 1983).

14. Kato, C., et al., "On the Mechanism of Corrosion of Cu-9.4Ni-1.7Fe Alloy in Air Saturated Aqueous NaCl Solution I. Kinetic Investigations," Journal of Electrochemical Society, Vol. 127, No. 9 (Sep 1980).

15. Tomashov, N.D., "Theory of Corrosion and Protection of Metals," The Science of Corrosion, MacMillan Company, New York, p. 236-247 (1966).

INITIAL DISTRIBUTION

Copies		Copies	Code
2	ONR	1	28 (Belt)
7	NAVSEA	3	2803 (Montemarano)
	1 SEA 05		
	2 SEA 05R25	1	2809
	2 SEA 05M1		
	2 SEA 99612	5	281 (Wacker)
12	DTIC	15	2813 (Morton)
		10	2813 (Scully)
		1	TIC
		2	5231 (Office Services)

DTNSRDC ISSUES THREE TYPES OF REPORTS

1. DTNSRDC REPORTS, A FORMAL SERIES, CONTAIN INFORMATION OF PERMANENT TECH-
NICAL VALUE. THEY CARRY A CONSECUTIVE NUMERICAL IDENTIFICATION REGARDLESS OF
THEIR CLASSIFICATION OR THE ORIGINATING DEPARTMENT.

2. DEPARTMENTAL REPORTS, A SEMIFORMAL SERIES, CONTAIN INFORMATION OF A PRELIM-
INARY, TEMPORARY, OR PROPRIETARY NATURE OR OF LIMITED INTEREST OR SIGNIFICANCE.
THEY CARRY A DEPARTMENTAL ALPHANUMERICAL IDENTIFICATION.

3. TECHNICAL MEMORANDA, AN INFORMAL SERIES, CONTAIN TECHNICAL DOCUMENTATION
OF LIMITED USE AND INTEREST. THEY ARE PRIMARILY WORKING PAPERS INTENDED FOR IN-
TERNAL USE. THEY CARRY AN IDENTIFYING NUMBER WHICH INDICATES THEIR TYPE AND THE
NUMERICAL CODE OF THE ORIGINATING DEPARTMENT. ANY DISTRIBUTION OUTSIDE DTNSRDC
MUST BE APPROVED BY THE HEAD OF THE ORIGINATING DEPARTMENT ON A CASE-BY-CASE
BASIS.